# UNIVERSITÀ DEGLI STUDI DI PADOVA

Department of Geosciences

Master's Degree in
Geophysics for Natural Risks and Resources

# LOCAL SEISMIC RESPONSE ANALYSIS AND INTERACTION WITH HISTORICAL BUILDINGS: THE VERONA ROMAN THEATER CASE

SUPERVISOR:          PROF. JACOPO BOAGA

CO – SUPERVISOR:     PROF.SSA FRANCESCA DA PORTO

CANDIDATE:
ELEONORA RIGATO
n° 2045251

A.Y. 2022/2023

# INDEX

# *INTRODUCTION*

The city of Verona has been identified, from a seismic point of view, in zone 2, that is an area in which strong earthquakes could occur.

The aim of this thesis is to apply a multidisciplinary approach in the field of seismic protection of cultural heritage. The application takes place at the Roman Theater of Verona and provides for an integration between geophysical approach and the engineering one of the structural analyses. The four important steps for this study are at first a geological and geophysical analysis that provides information about the soil. Then a local seismic response analysis is performed, followed by a dynamic identification of the structure. At least kinematic and numerical computational models are used for the evaluation of the structures.

All these points will be treated in the following work; it is divided in five chapters: the first one gives general information about the study area, geological settings and the seismicity.

In chapter 2 are explained the geophysical methods used in the past to define the subsoil of the Roman Theater area, but also the geophysical surveys made in February 2023 with the purpose of having more detailed information of the different layers.

Chapter 3 shows the local seismic response analysis, that uses the information of the soil that characterize the site, in order to understand if it may amplify the seismic action. The results are useful to define the seismic action of the project, that is used to perform the structural analyses of the walls of the Roman Theater.

Starting from the fourth chapter the study is concentrated on the structure and on its structural behavior. At first a kinematic analysis is done, it consists in the evaluation of the local mechanism and the capacity of the structure to bear the request acceleration of the site.

In chapter 5 at first a dynamic identification is performed through an experimental and numerical approach. Based on the experimental results a numerical model of the theater was constructed and calibrated. Then on the calibrated model a linear dynamic analysis was performed to investigate the dynamic behavior of the structure. Depending on the characteristics of the soil and of the structure it is possible to obtain very different response.

Thanks to this thesis, it was possible to analyze a part of the Roman Theater in a complete way.

# *ROMAN THEATER: CASE STUDY*

The Roman Theater is the most important theatre in Verona and was built around I century BC. This is on the left bank on the Adige River and for the edification was developed the slope of San Pietro hill. This choice provides "*the opportunity to act as a support for the tiers of the auditorium and to create a terraced scenography solution.*" [Da Porto et al, 2022] (*Figure 1.1*).



**Figure 1.1** - *Position of the study area in Verona*

The construction of the theatre occurred during the Augustan age and this may be understand by the architectural features used (*Figure 1.2*). The structure took many years to build, due to its great size: about 150m wide in the part near the river, 107m in the inner part and 100m long. The scene area is 71,50m long and the stage 59,50m. It is characterized by an altitude difference of 70m.

*Figure 1.2* - Model of Roman Theater after construction

In past, the theatre was affected by a series of natural disaster:

- 589: flood of Adige River caused damages to the *postcenium* and to the scene area
- 793 and 1117: two big earthquakes that caused the collapse of the theatre walls
- 1195: flood of Adige River caused damages to foundation of theatre

The current state of the structure is composed by 5 radial walls in the eastern part and 4 in the western one. The entrance structure with arches and the structure of the scene in the southern area, corresponding to one third of the original building in height (*Figure 1.3*).



*Figure 1.3* - Current conditions of Roman Theater

The structure is made in tuff, extracted by San Pietro hill. This is a yellowish gray marly sandstone, also called Marne di Priabona. This is a stone resistant to compression and easy to cut. In some parts of the structure also the ammonite limestone from Valpolicella quarries was used. The disadvantage of the marly sandstone is that it degrades quickly outdoors. Indeed, the different elements of the theatre present several degraded parts (*Figure 1.4*).



*Figure 1.4a* - *Internal view of the stage building*



*Figure 1.4b* - *Western radial wall of the cavea*

***Figure 1.4c*** *- Western radial walls of the cavea*

Particular attention was paid to infiltration waters, "*since the building occupied the slope of a hill made up of a stone of low hardness*" [Da Porto et al, 2022]. The rocky substratum, of calcareous-limestone nature, is a type of rock subjected to karst phenomena. This means that the waters move from the summit areas through a series of fractures and to control these, in the past, was built a water collection trench that today does not work due to poor maintenance activities.

The theatre is one of the most important buildings of the Roman ages in Verona. It is characterized by a high vulnerability and a poor conservation of materials. The partitions can be considered as free elements subjected to possible activation of local collapse mechanisms.

## 1.1 Geological setting

From a geological point of view the study area is situated in a transition zone between a hilly-mountainous area and a high plain area. Indeed, *"[…] the Lessinian hilly context is characterized by broad ridges which gradually fan out until the outlet in the Upper Plain and whose slopes, generally with medium steepness, appear to be furrowed by more or less pronounced torrential incisions.*" [2]. In particular, "*the site of interest is located on the slopes of a secondary hilly ridge which from Castel San Felice extends in a North North-East – South South-West direction up to Colle San Pietro, finally stopping close to the course of Adige River*" [Valdinoci et al, 2022] (*Figure 1.5*).

6

***Figure 1.5*** – *Panoramic photo seen from the south. The site of investigation is in red*

The lithologies that are around Verona are rocky lithotypes with calcareous-calcarenite facies of Tertiary. As indicated in the "*Carta geologica del territorio del Comune di Verona*" (*Figure 1.6*) the outcropping lithology is the Marne di Priabona (Upper Eocene), composed by greenish-grey clayey marls or limestones with intercalations of calcarenites and organogenic limestones. In the upper part this lithology is altered and the stratification is difficult to distinguish. On the surface of build-up area and in the study area there are also levels of heterogeneous reworked material. This type of material is the result of different anthropic activities and is composed by a highly variable percentage of silty-sandy component where the elements have different granulometric characteristics. This coverage level has variable thickness and poor lateral continuity. As will be shown in 2, the coverage layer has a thickness that changes from the northern area to the southern one: this goes from 1m to 9m of depth.

1 - Colluvial and eluvial materials covering the slopes.

2 – Current and recent mainly sandy-silty alluvial of Adige Rivers modeled in the Würmian bed.

4 – Valley floor alluvial mainly: silty (l), gravelly and pebbly (c).

5 – Predominantly silty-clayey colluvial deposits of the lateral valleys that join up with the alluvial valley floor. Fine deposits of suspended valleys. Predominantly fine colluvial deposits of the foothills, sometimes with coarse detrital skeleton, mainly as a function of the lithological nature of the slope.

6 – Terraced fluvioglacial and fluvial alluvial of the ancient fan of the Adige River, gravelly and pebbly (c); Loess cover (lo); Würm (W).

7 – Terraced fluvioglacial and fluvial alluvial of the ancient fan of the Adige River, sandy (s); gravelly and pebbly (c); Riss (R).

8 – Calcarenites with pectinids and large melobesias; biocalcarenites; fine yellowish sandstones more or less rich in pebbles calcareous. Middle Miocene p.p. (Serravallian p.p. – Langhiano).

9 – Marne di Priabona. Clayey limestones, marls and subordinately discocycline limestones, generally stratified indistinct; melobesia calcarenites. Upper Eocene (Priabonian).

Terrace edge in fluvioglacial or fluvial deposits.

Establishes and presumed faults.

Well of water.

Trace of geological section.

*Figure 1.6 - Off-scale extract of "Carta geologica del territorio del Comune di Verona" 1:20 000. The study area is highlighted with red circle*

## 1.2 Structural and seismic setting

The Veneto region is subdivided in seismic district, where "*each district represents an area inside which earthquakes can be identified by some common seismogenic elements.*" [Sugan et al, 2011]. The case study is inside the Lessini-Schio district, defined by the letter L (*Figure 1.7*).
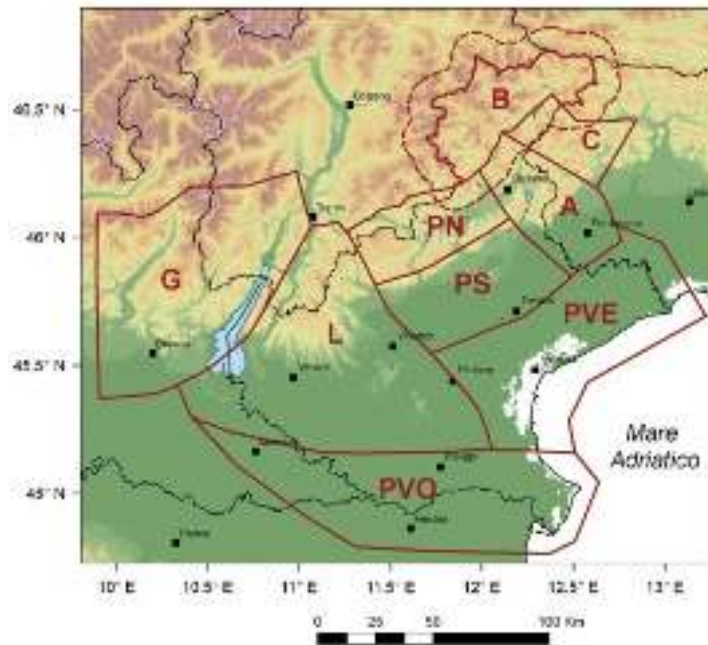


*Figure 1.7 - Seismic district in the Veneto region: Giudicarie (G), Lessini-Schio (LS), Pedemontana Sud (PS), Pedemontana Nord (PN), Alpago-Cansiglio (A), Claut (C), Alto Bellunese-Dolomiti (B), Pianura Veneta Est (PVE), Pianura Veneta Ovest (PVO)*

To describe the neotectonics of the study area is used the "*Database of Individual Seismogenic Sources*" that is a database in which all the seismogenic sources are present on the basis of seismic and geological studies. Three different types of seismogenic sources can be identified:

- Individual seismogenic sources: known or suspected structure associated with a significant earthquake

- Composite seismogenic sources: based on geological data and are not associated to earthquakes

- Debated seismogenic sources: source hypothesis on which there is still no interpretative agreement

The study area is ubicated inside a debates seismogenic source, called "ITDS075 – Sant'Ambrogio" (*Figure 1.8*). Going into more details, near the Teatro Romano there are some capable faults, these are *"[…] structures that have generated surface faulting in the last 40,000*

*years and are therefore considered potentially capable of creating new deformations on the surface.*" [Valdinoci et al, 2022] (*Figure 1.9*).
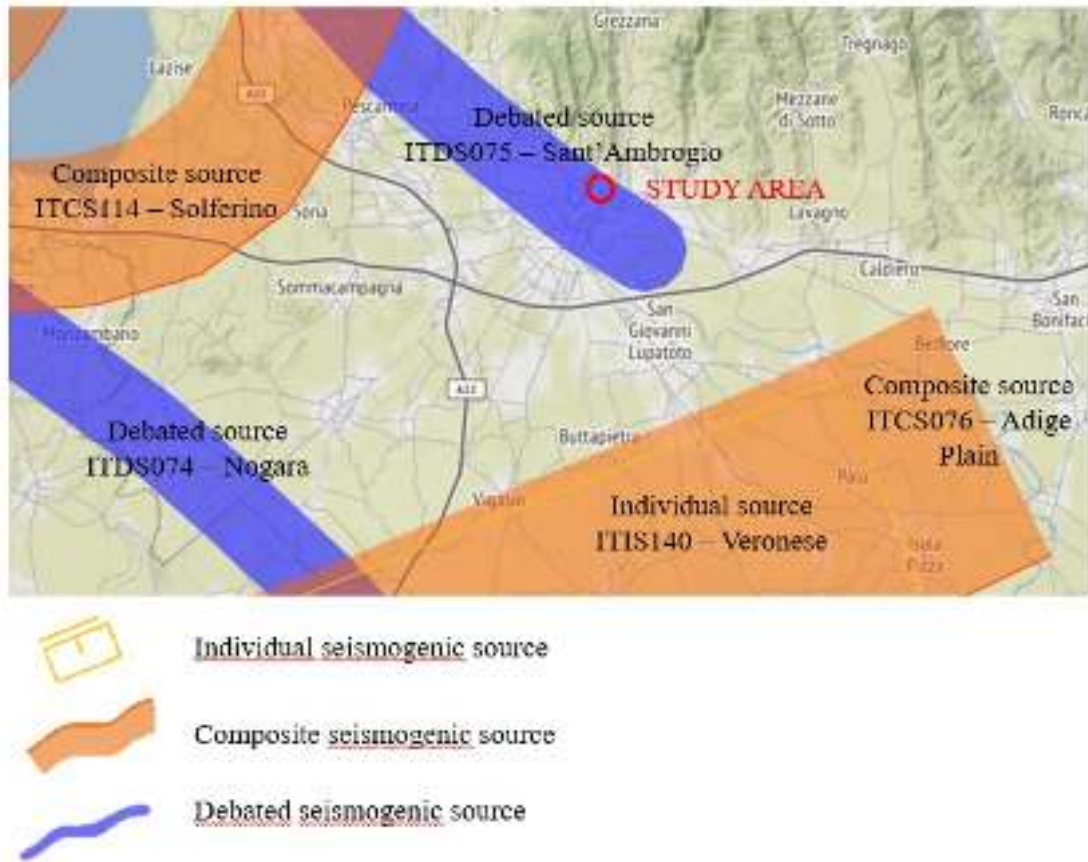


*Figure 1.8 - Out of scale image from "Database of Seismogenic Sources" where the study area is highlighted with the red circle*
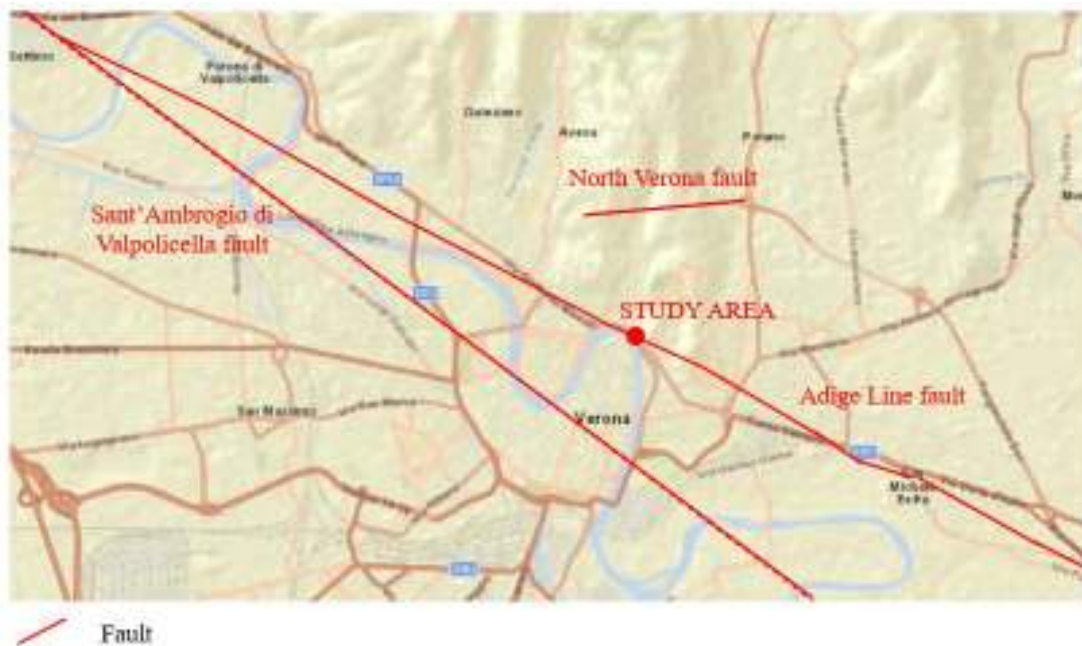


*Figure 1.9 - Capable faults in near the study area from the "Catalog of capable faults - ITHACA". The red circle highlights the study area*

In *Figure 1.9* are marked three faults that represent:

- North Verona Fault: this is a normal fault that is 1,5km North to the study area and its latest activities were recorded during the Holocene (< 10.000 years ago)
- Adige Line: it has a length of 35km with NW-SE orientation. This feature is located in the vicinity of the study area and has been characterized by activity up to historical times (< 3000 years ago)
- Sant'Ambrogio di Valpolicella fault: strike-slip fault with the last activity during the Pleistocene.

During 1117, in Verona occurred one of the biggest earthquakes recoded with a magnitude of $M_w = 6.49$. The source and the damages of this earthquake are uncertain. Today the source is associated to the Adige Plain, which is also defined as the maximum seismogenic potential for the Lessini-Schio district. This could generate earthquakes up to a magnitude of 6.7.

# *GEOPHYSICAL SURVEY*

The purpose of applied geophysics is to provide a characterization of the subsurface regarding the geology, geological structures, groundwater and contamination. The geophysical methods for the subsoil exploration investigate two different aspects of the subsoil:

- Structure: that means the geometry of the subsoil
- Dynamic: how the subsoil changes during the time

These methods can be divided in two different groups: active and passive. The active methods are methods in which there is a controlled source and the receivers record a variation of a certain physical parameter. The second ones are methods that do not require an energization and all the data are acquired from the natural variations of the physical parameter. The geophysical methods can be divided also in invasive and non-invasive methods, where the first consists in the use of boreholes into the ground.

In the study area were made different investigation to characterize the subsoil. For this work two different methods were used: Multichannel Analysis of Surface Waves and Horizontal to Vertical Response Ratio. In the past, other surveys have been carried out that are the continuous core survey and the electrical method. The last two will be addressed in the first part of the chapter to have a comparison between the data obtained from the recent acquisition and a complete characterization of the subsoil.

## 2.1 Geognostic survey of the 2000s

In April 2000, different geognostic and geophysical surveys were made inside the Roman Theater. Two continuous core survey and four vertical electric survey were carried out and the depth of investigation is about 20m. In *Figure 2.1* is possible to see the position of the different acquisitions, where the core surveys are defined with S1 and S2, otherwise the vertical electrical survey with SEV1, SEV2, SEV3 and SEV4.
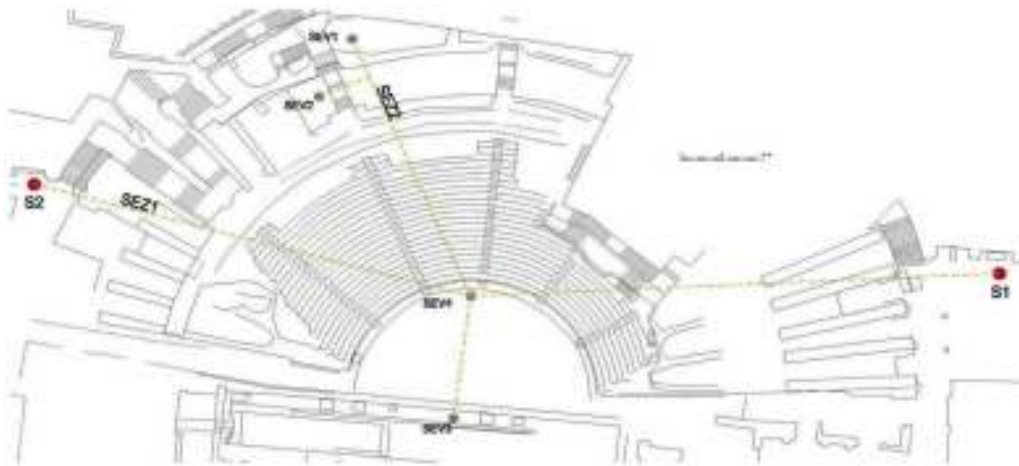
***Figure 2.1*** *- Position of geognostic and geophysic acquisitions. The core surveys are identified with S1 and S2. The vertical electrical surveys are identified with SEV1, SEV2, SEV3, SEV4*

From the drilling is showed that the soil is characterized by different layers: the first one is a silty sandy gravel with different depth indeed in S2 the second layer is a depth about 1,10m while in S2 at 9m of depth. Below the gravel there is organogenous calcarenite (*Figure 2.2*). With the electric survey is investigated the bedrock and its trend. From the surveys is shown that the first layer has a higher resistivity. About the bedrock, this changes its thickness and in SEV3 it reaches a depth about 8m.
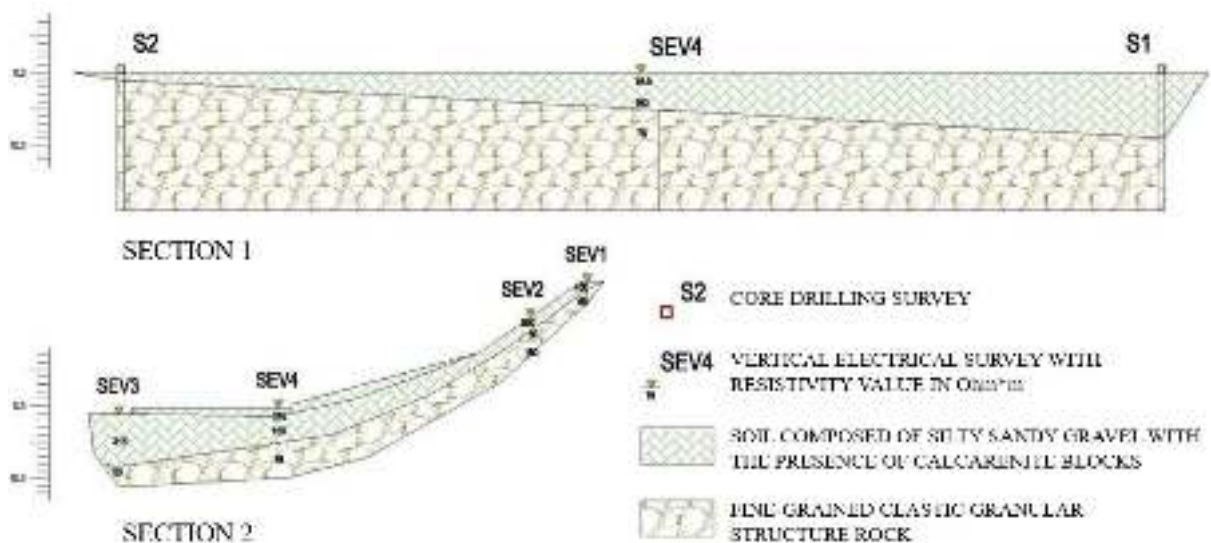


***Figure 2.2*** *– Sections resulting from drilling and vertical electric survey*

## 2.2 Electric method

In 2019 other geophysical investigations were made at the Roman Theater, including the electric methods. This survey is made with the aim to define the subsoil from an electric point of view. It investigates both aspects of geophysics: structure and dynamic. The physical property that is measured is the electrical resistivity.

### 2.2.1 Physical principles of electric methods

The ERT is a direct current electric method based on Ohm's law:

$$\Delta V = R \, I$$

Where $\Delta V$ is the electric potential difference, I is the injected current and R is the resistance. The resistance depends on the material and on its dimensions:

$$R = \frac{\rho \, L}{A}$$
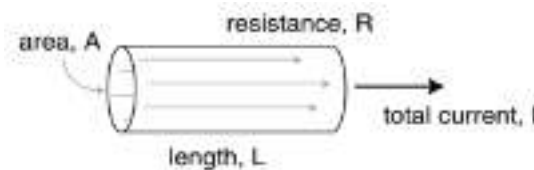


**Figure 2.3** - *Current flows a material*

$\rho$ is the electrical resistivity that represents the ability of a material to resist the flow of current. This method consists in the injection of a current in the ground and the effect observed is a voltage changing. What is measures is the apparent resistivity that is given by the resistivity multiplied by a geometric factor:

$$\rho_a = \frac{V \, k}{I}$$

The geometric factor takes in consideration the geometry of the system. To obtain the real value of resistivity an inversion is required.

### 2.2.2 Survey configuration and field acquisition

For this survey a Wenner array is used, this type of array has the potential electrodes in the middle and the current electrodes at the edges, the distance between each one is the same (*Figure 2.4*). The advantage of this configuration is a higher depth of investigation and higher intensity of the signal.
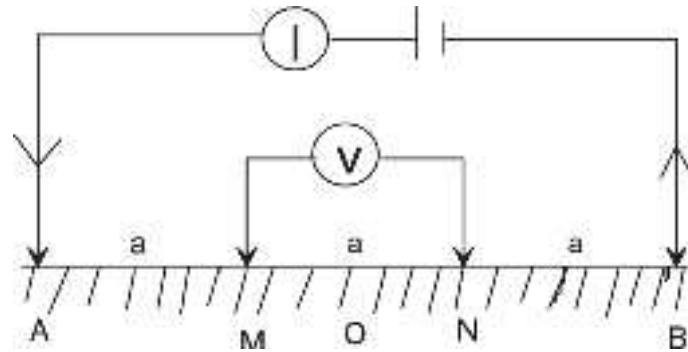
***Figure 2.4*** *- Wenner array. M and N are potential electrodes, A and B are current electrodes, a is the distance*

In this survey 2 different acquisition were made, both with 24 electrodes but in line 1 the distance between the electrodes is 1m and in line 2 the distance is 1,5m (*Figure 2.5*).
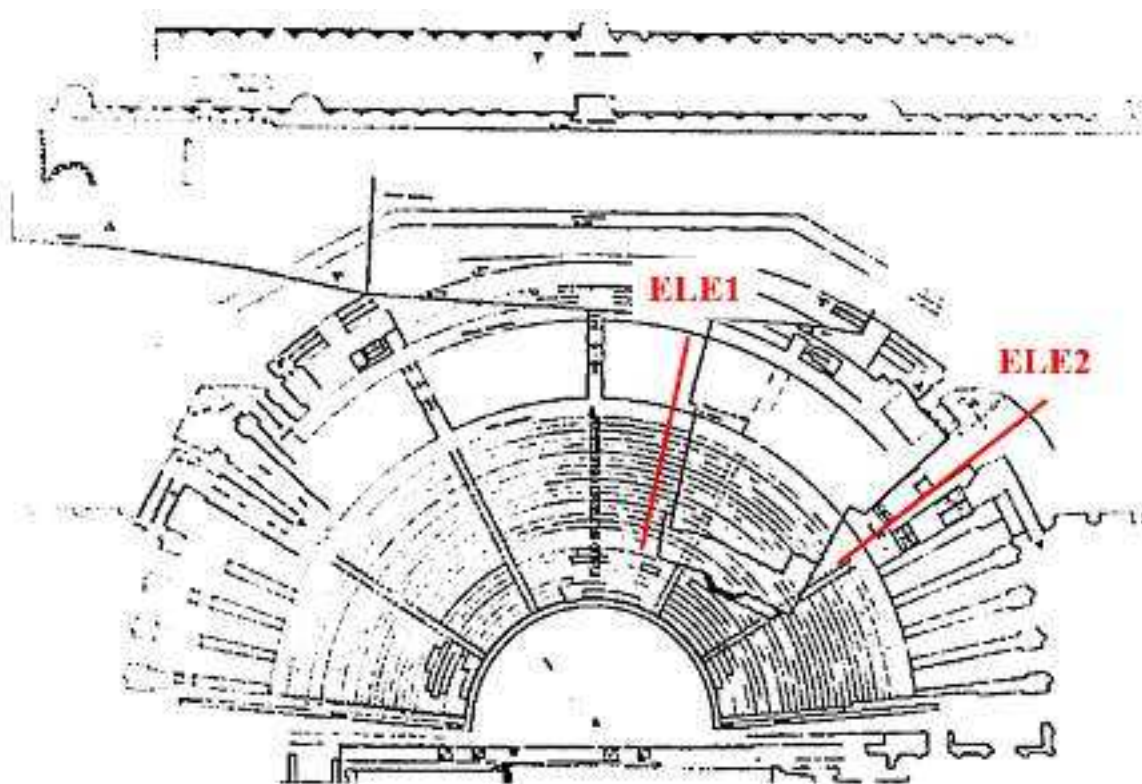


***Figure 2.5*** *– Position of ERT surveys*

## 2.2.3 Results

The results obtain from line 1 show the presence of an upper layer with a higher resistivity, > 300 – 500 Ohm*m. Below this one the resistivity is typical of conductive soil with a resistivity that goes from 50 to 100 Ohm*m (*Figure 2.6*).

The line 2 shows lower value of resistivity (< 200 Ohm*m) and two anomalies with high resistivity were found. The first is near a retained wall, the second is a void (*Figure 2.7*).
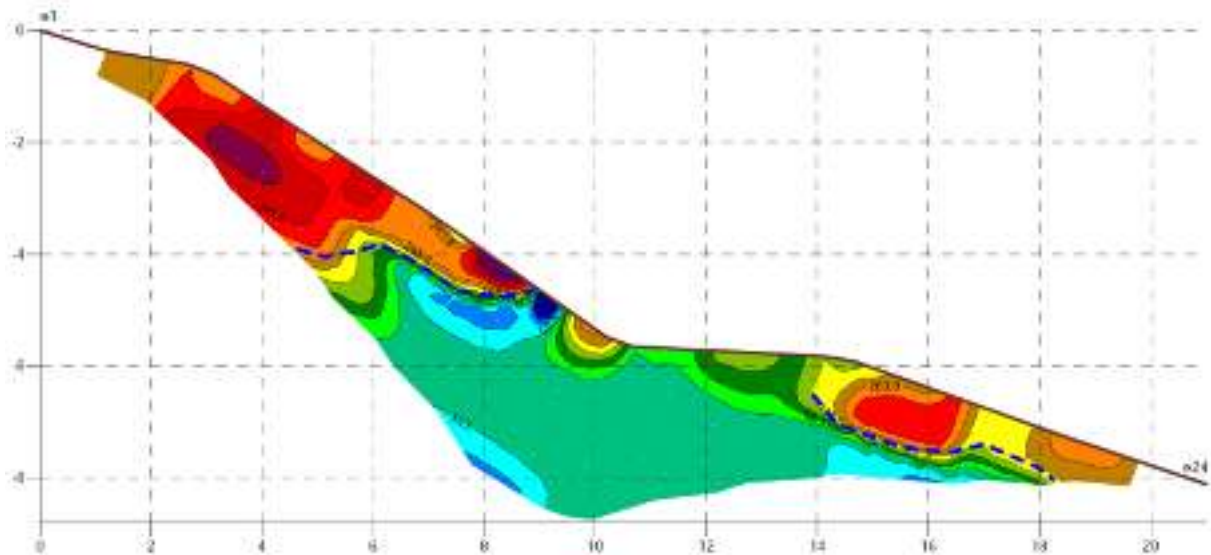
*Figure 2.6 - Result from ERT line 1*
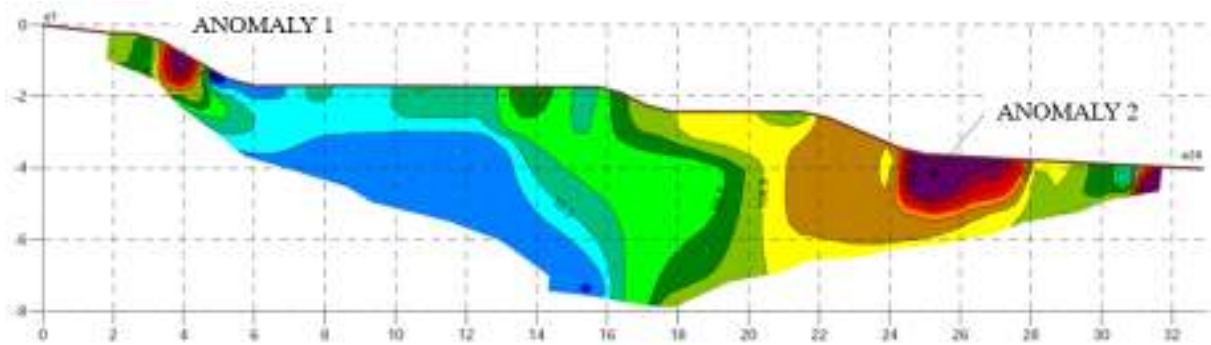


*Figure 2.7 - Result from ERT line 2*

## 2.3 Multichannel Analysis of Surface Waves

The Multichannel Analysis of Surface Waves, also called MASW, is a seismic method that uses surface waves to retrieve the velocity profile of S-waves. MASW is the most used to retrieve the S-waves velocity because the seismic method with S-waves requires horizontal geophones and a source that can produce shear waves.

This is a no invasive method with a controlled source. This method exploits the dispersive characteristics of surface waves. The Rayleigh waves are the most used and are easy to generate and to record. From the spectral analysis of surface waves can be retrieved a dispersion curve that is used to obtain the velocity-depth profile of the shear waves.

### 2.3.1 Physical principles of seismic methods

The aim of this method is to investigate the structure and to obtain the best image possible of the subsoil. The physical parameter that are considered in this case are the elastic properties of the media: elastic moduli and density. The study of wave elastic propagation in the subsoil furnishes the mechanical parameters of it.

When the subsoil is subjected by an energization, like a shot with a hammer or a weight drop, there is a reaction that consists in a stress-strain relation (*Figure 2.8*).
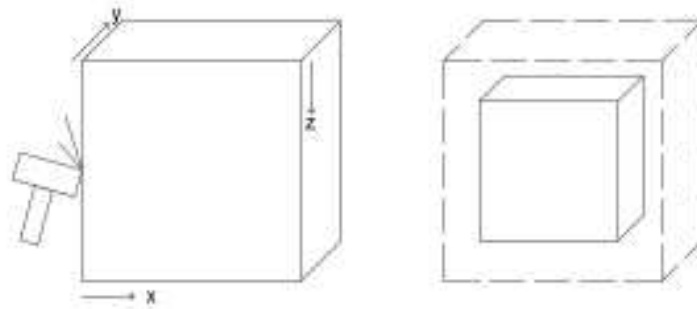


***Figure 2.8*** *- Deformation of a cube*

$\varepsilon$ is the strain that represents the variation along the direction u, v, w (displacement in x, y, z). If there is a variation, the strain that can be observed in the 3 directions is given by:

$$\varepsilon_{xx} = \frac{du}{dx}$$

$$\varepsilon_{yy} = \frac{dv}{dy}$$

$$\varepsilon_{zz} = \frac{dw}{dz}$$

The sum of the three different strains gives the dilation, also called dilatation:

$$\Delta = \varepsilon_{xx} + \varepsilon_{yy} + \varepsilon_{zz}$$

The Hooke law for isotropic media is:

$$\sigma_x = \lambda\Delta + 2\mu\varepsilon_y$$

Where the pure shear stress is:

$$\sigma_y = \mu\varepsilon_y$$

$\lambda$ and $\mu$ are the Lamé constant that are mechanical constant, where $\lambda$ is associated to the compression and $\mu$ to the shear.

Suppose now to re-write Newton's law F = ma in an infinitesimal way, knowing:

$$dm = \rho \, dx \, dy \, dz$$

The result is the Newton's law applied to a fixed element and this is:

$$\rho \frac{d^2 y}{dt^2} = \frac{d\sigma_{xx}}{dx} + \frac{d\sigma_{yy}}{dy} + \frac{d\sigma_{zz}}{dz}$$

So, the Hooke's law can be written as:

$$\rho \frac{d^2 u}{dt^2} = (\lambda + \mu)\frac{d\Delta}{dx} + \mu \Delta^2 u$$

The result is the wave equation, that consists in a differential equation:

$$\rho \frac{d^2 u}{dt^2} = (\lambda + 2\mu)\nabla^2 u$$

where $\nabla$ is the Laplacian operator which indicates the divergence of the gradient of a function on Euclidean space. The wave equation says that different media reacts in a different way with the same force.

In seismic are not used $\lambda$ and $\mu$ but are used the bulk modulus k and the shear modulus G, that are respectively given by:

$$k = \lambda + \frac{2}{3}G$$

$$G = \mu = \rho \, v_s^2$$

The solution of the wave equation are the body waves: P-waves and S-waves. To retrieve the solution for the P-waves the divergence must be applied:

$$\rho \, \nabla \cdot \frac{d^2 u}{dt^2} = (\lambda + 2\mu)\nabla^2 (\nabla \cdot u)$$

$$\frac{d^2}{dt^2}(\nabla \cdot u) = \frac{(\lambda + 2\mu)}{\rho}\nabla^2 (\nabla \cdot u)$$

The velocity of P-waves is inside the equation and is given by:

$$v_P = \sqrt{\frac{\lambda + 2\mu}{\rho}}$$

P-waves are compressional waves and represents the divergence of the displacement. These oscillate in the same direction of the propagation and produce a change in volume (*Figure 2.9*). These propagate both in solids and liquids and are the first that are recorded in the seismogram during an earthquake.
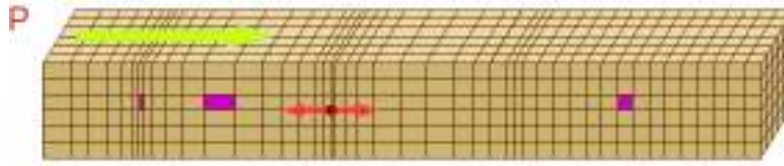


**Figure 2.9** - *Propagation of P-wave*

About the S-waves, to find the solution the curl must be applied:

$$\rho \frac{d^2}{dt^2} (\nabla \times u) = \mu \nabla^2 (\nabla \times u)$$

$$\frac{d^2}{dt^2} (\nabla \times u) = \frac{\mu}{\rho} \nabla^2 (\nabla \times u)$$

The velocity of S-waves is given by:

$$v_S = \sqrt{\frac{\mu}{\rho}}$$

S-waves are transversal waves and have an oscillation that is perpendicular to the direction of propagation (*Figure 2.10*). These waves do not propagate in the fluids and are slower than P-waves:

$$v_P \approx 1.9\, v_S$$
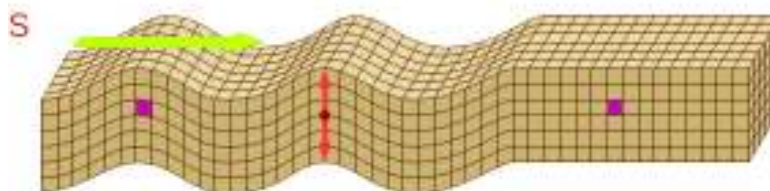


**Figure 2.10** - *Propagation of S-wave*

Then, there are the surface waves which are not body waves but are generated from the constructive interference of P and S waves. The surface waves are the Rayleigh waves that are characterized by an elliptical motion and the Love waves that are S-waves polarized in surface

(*Figure 2.11*). These waves are slower than the other but are the more dangerous during an earthquake.
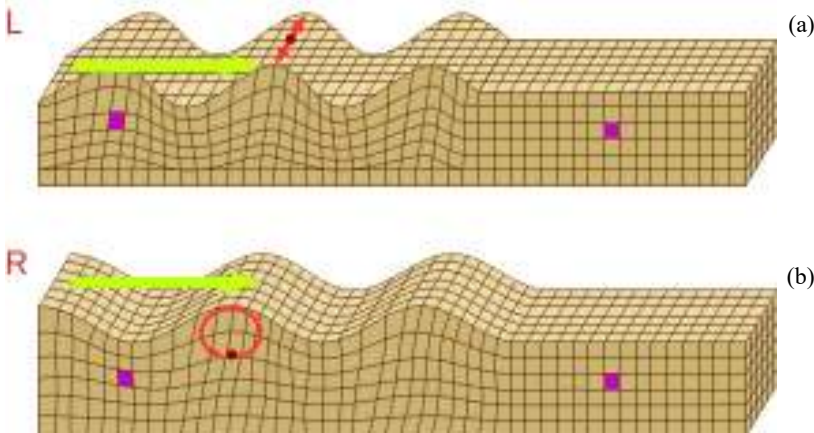


*Figure 2.11 - (a) Love wave propagation; (b) Rayleigh wave propagation*

Surface waves are characterized by a lower attenuation. Indeed, the body waves have an attenuation that is 1/r respect to the surface waves that attenuate as 1/r $^{0,5}$. This explains why at large distances the SW amplitudes are greater than body waves. These waves are the more energetic ones and have low frequencies. Low frequency permits to the wave to go deeper in the subsoil. This type of waves is dispersive that means each frequency is characterized by a different velocity and for this, different wavelets insist in different parts of the soil: waves with lower frequencies go deeper than the high frequencies that stay in the upper part of the subsoil (*Figure 2.12*).
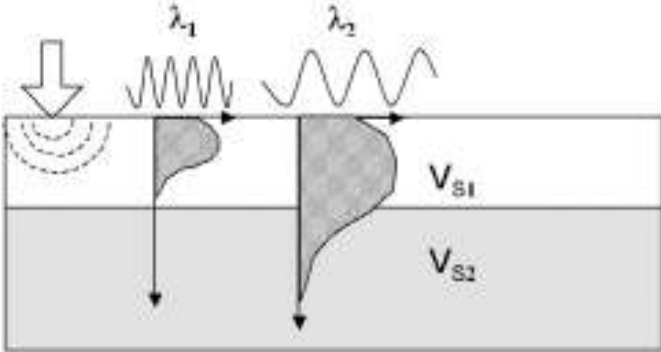


*Figure 2.12 - Schematic representation of geometric dispersion of Rayleigh waves: the vertical displacement associated with a short and a long wavelength*

### 2.3.2 Survey configuration and field acquisition

Inside the Roman Theater are made surveys with the MASW technique in 2 different positions of the theatre (*Figure 2.13*). The aim of this investigation is to find the different lithologies to obtain the properties and the parameters ($v_s$, $v_p$, density, shear modulus, damping).
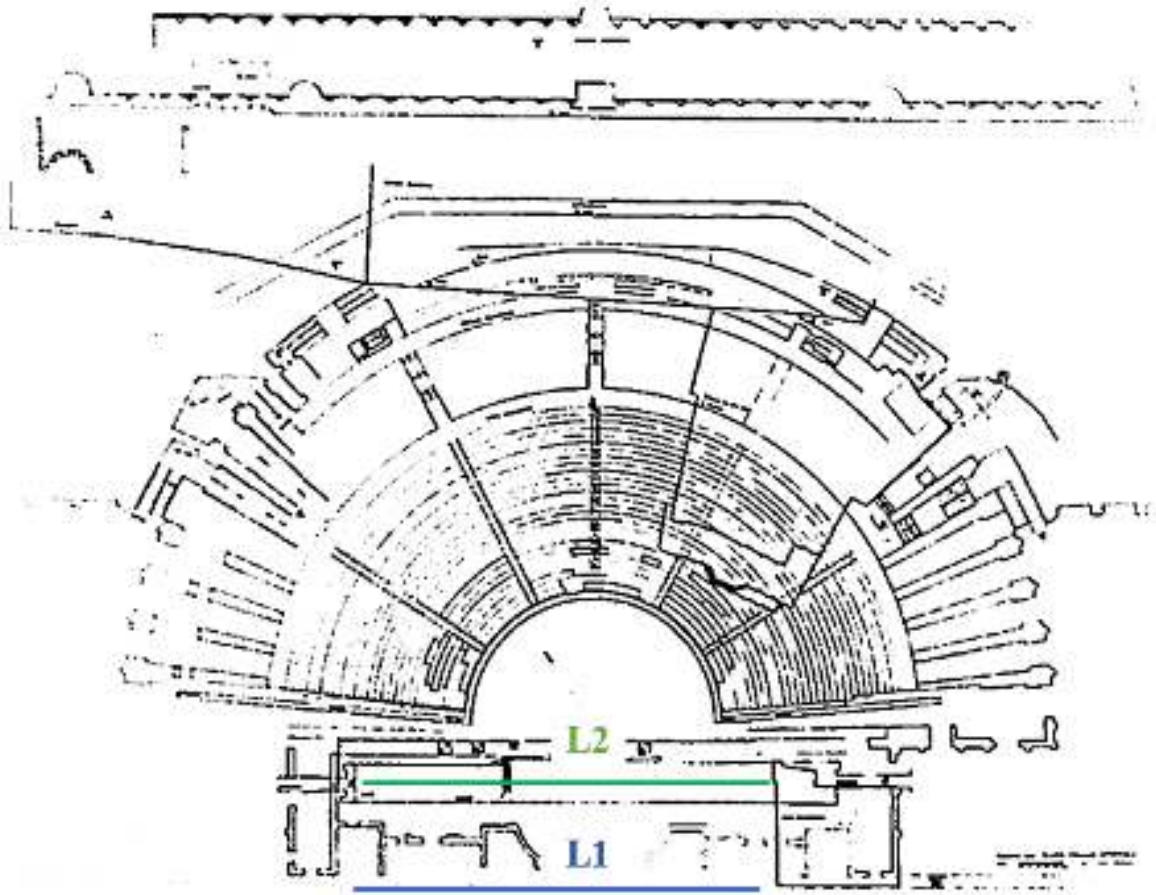


***Figure 2.13*** *- Position of MASW acquisition inside Roman Theater*

The acquisition of the data consists in a multichannel analysis, using 48 geophones with the following spatial and temporal configuration.

***Table 2.1*** *– Acquisition parameters of MASW inside Teatro Romano*

| MASW survey | |
|---|---|
| Seismic source | Weight drop – 50 kg |
| Number of geophones | 48 |
| Total length | 48 m |
| Spacing interval | 1 m |
| Sampling interval | 0,25 ms |

As is reported in the *Table 2.1*, the source that is used is a weight drop that is released at a height of about 2 m (*Figure 2.14*). In the case of this type of source usually is used a metal plate, this for 2 reasons: the first one is to avoid the formation of a hole, when the mass hits the ground, that consists in a loosing of plastic energy and to have the time zero that corresponds to the time in which the measuring starts.



**Figure 2.14** - *Weight drop used for the acquisition*

To acquire the signals were used the geophones (*Figure 2.15*). These are device that converts the ground movements into a voltage: they generate an electric signal that is proportional to the particle velocity.



**Figure 2.15** - *Geophones used during field acquisition*

All the sensors were connected to a cable and the measuring device was in the middle of the array, between geophones 24 and 25.

For each line were made several measurements and in different position of the array. For line 1 were made 30 measurements, where the first measurement was made out of array at a distance of 11m from geophone 1. The second was at the geophone 1; then, the last ones at 1m of distance from geophone 48. During the acquisition was found that the geophone 12 did not work in a good way, probably due to a malfunction of the geophone itself.

About line 2, the position of the source during the acquisition was at geophone 1 and at geophone 46.

Taking a first look at the area, probably the acquisition of line 2 will be better than the acquisition of line 1 for two reasons. The first one because the geophones were in a soil that is characterized by rock material and archeological remains that reduce the galvanic contact (*Figure 2.16*). The second reason is that line 1 is very close to the street, so the noise during the acquisition is very high.



***Figure 2.16*** *- Presence of archeological remains near line 1*

### 2.3.3 Processing

For the processing of the data a MATLAB code provided by prof. Jacopo Boaga was used. During the field acquisition the measuring device creates a SEG-2 format file for each measuring, which will be the input inside the code for the processing.

The SEG-2 file is a format file that is mainly used for raw or processed shallow seismic data. The structure of this file includes:

- File Description Block: provides information requires to parse the rest of the overhead data and other information common to all traces in the file

- Trace Description Block: provides location, format and other information

- Data Block: consists of fixed point or floating point number

After the import of the file and the spatial and sampling interval are defined the first output is the seismogram of raw data (*Figure 2.17*). This seismogram shows energy only in a certain part and in the rest, there is no energy. For this reason, is better to normalize the seismogram (*Figure 2.18*), that consist to look to the maxima for each sensor in terms of amplitudes and normalize them. The seismogram with raw data is useful to see the position of the source.
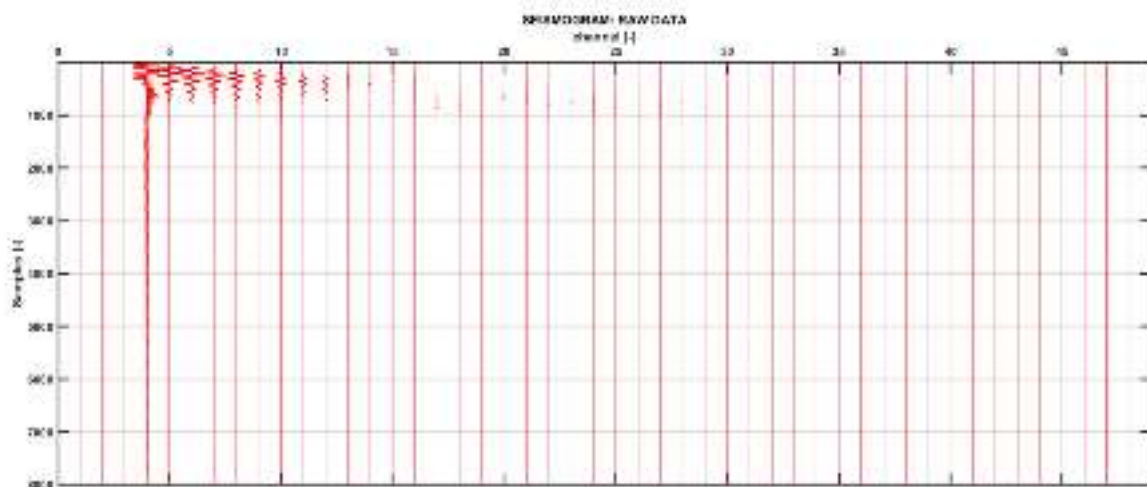


***Figure 2.17*** *- Seismogram of raw data of measure #35*
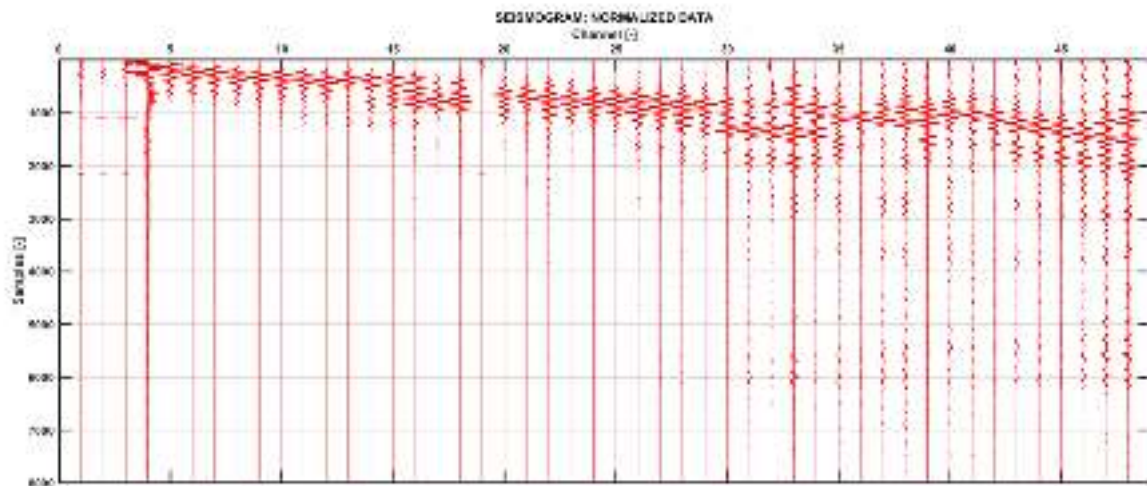
***Figure 2.18*** *- Seismogram of normalized data of measure #35*

After that, a spectral computation of the data is done. This consists in a 2D Fourier transformation that decomposes the signal in a sum of sinusoidal waves with different frequencies, amplitudes and phases. Indeed, with this pass from t-x domain (time-space domain) to f-k domain (frequency-wavenumber domain). Then, the frequency-phase spectra are plotted and through a manual picking there is the possibility to retrieve the dispersion curve (*Figure 2.19*). The result is the dispersion curve of the fundamental mode that is the input for the inversion process (*Figure 2.20*).
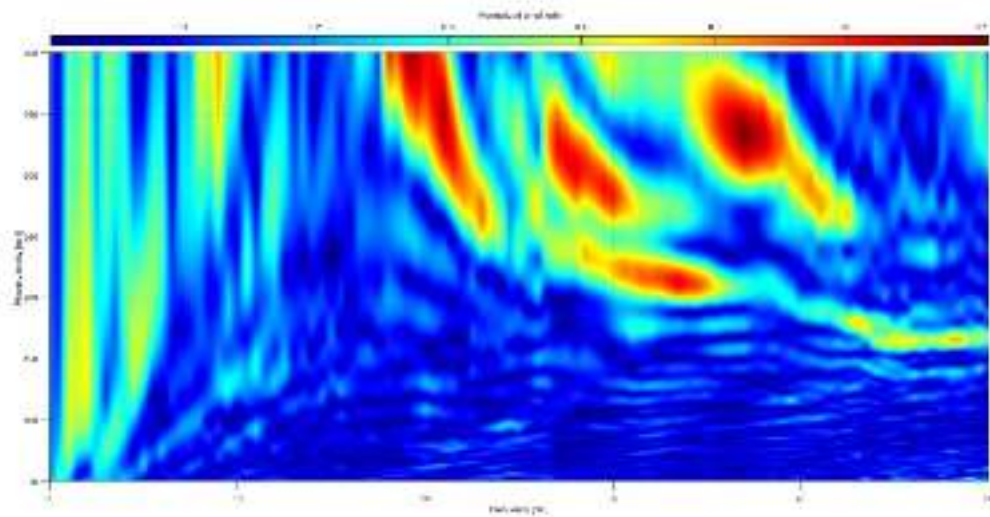


***Figure 2.19*** *- Frequency - phase spectra of measure #35*
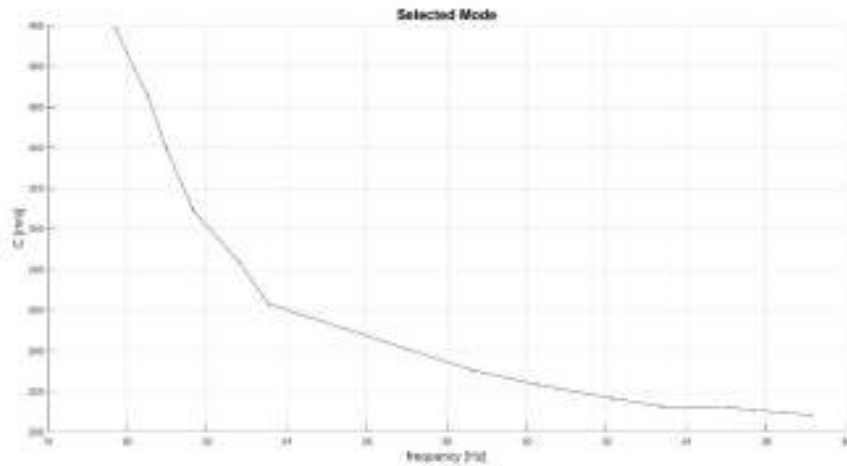
***Figure 2.20*** *- Dispersion curve of measure #35*

The next step of the code is to perform the inversion to obtain the $v_s$ depth profile of the area, obtained with the SWAMI code (Rix & Lai, *Figure 2.21*).
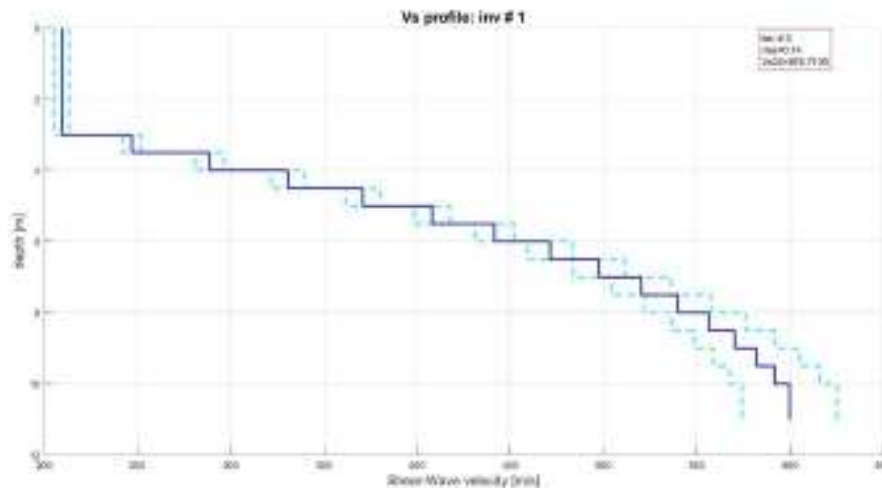


***Figure 2.21*** *- $v_s$ depth profile of measure #35*

## 2.3.4 Results

Only some $v_s$ profiles are taking in consideration, this because not all the acquisitions give clear results (*Figure 2.22*). Looking at these it is possible to distinguish two different layers and this is in according with the results discussed in the previous paragraphs. The first layer is a silty sandy material with a velocity around 250 m/s. The second one is a calcarenite with a higher velocity.
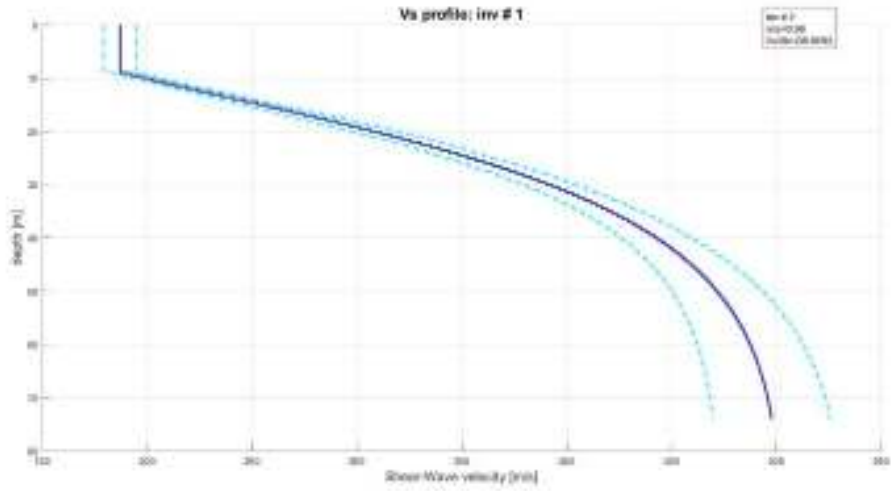
**Figure 2.22a** - *vs depth profile of measure #6*
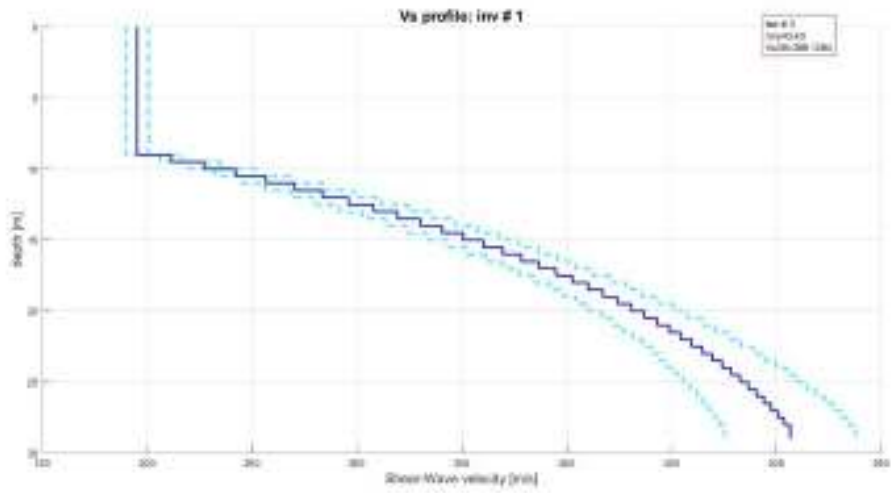


**Figure 2.22b** - *vs depth profile of measure #21*
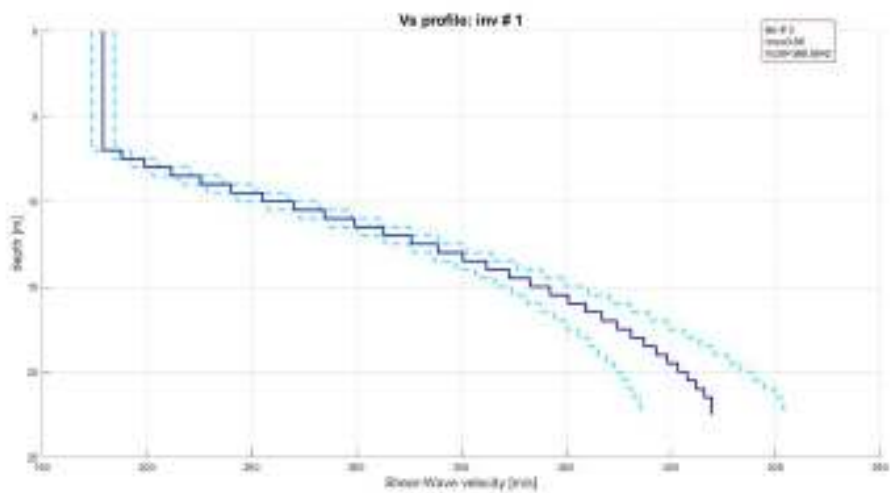


**Figure 2.22c** - *vs depth profile of measure #22*
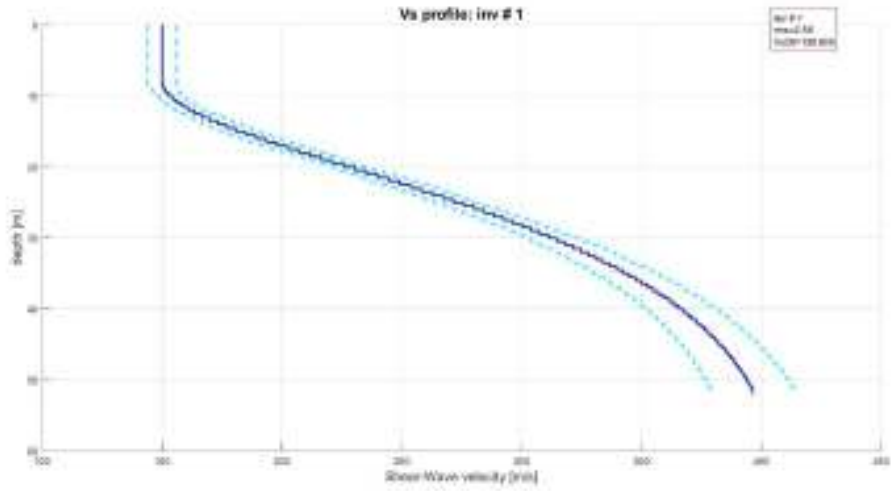
***Figure 2.22d*** *- vs depth profile of measure #28*
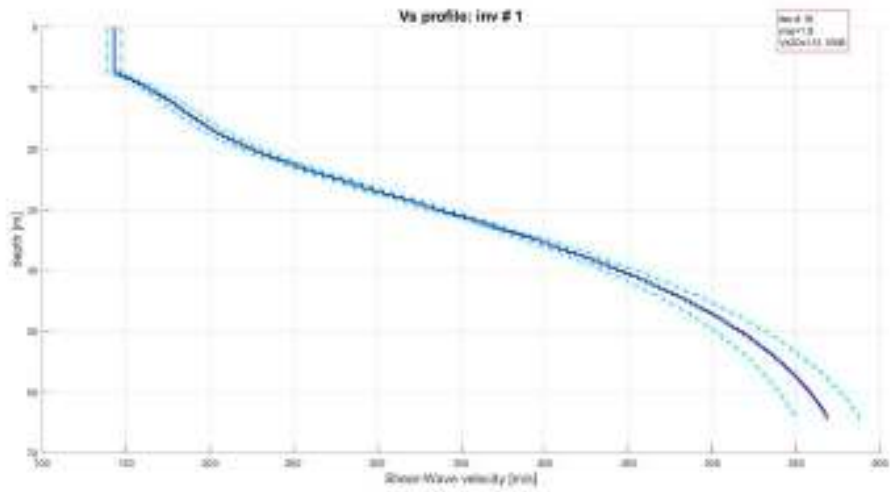


***Figure 2.22e*** *- vs depth profile of measure #32*
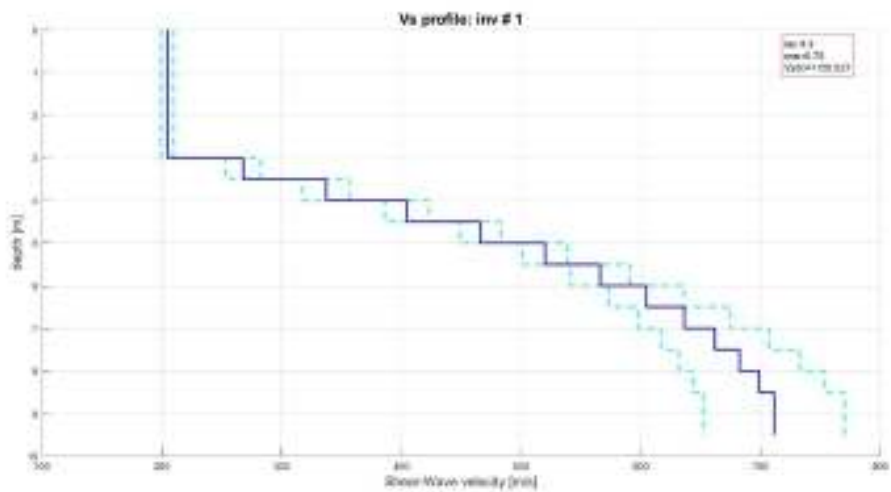


***Figure 2.22f*** *- vs depth profile of measure #34*

The summarized characteristics of each layer are reported in *Table 2.2*

*Table 2.2 – Characteristics of each layer*

|  | $V_s$ (m/s) | Depth (m) |
| --- | --- | --- |
| Silty sandy gravel | 250 | 0 – 8 m |
| Fine-grained clastic material | 700 | 8 – 20 m |

## 2.4 Horizontal to Vertical Seismic Response Ratio

The horizontal to vertical response ratio, also called HVSR, is a passive and non-invasive technique that measure the seismic noise in vertical and horizontal directions. The theory is related to the traditional seismic and to the theory of microtremors. The shape of the signal that is recorded depends on: the shape of the wave produced by the source, the path of the signal and the instrument response. This method records the seismic noise, that is generated by atmospheric phenomena and anthropogenic activity. It can be defined as microtremors because these signals are very small oscillation, smaller than the ones produced during an earthquake. This method, through the ratio between the horizontal and the vertical components in the frequency domain, can give different information:

- Resonance frequency of the sites: this is a fundamental parameter, depends on the thickness and on the rigidity of the soil and is very important to study from an engineering point of view.

$$f = \frac{(2n - 1)\, v_S}{4\, H}$$

H is the thickness of the layer, $v_s$ is the shear wave velocity and n is the mode number. In these cases, usually the mode of interest in the fundamental one (n=1) because is the most energetic, so the equation becomes:

$$f = \frac{v_S}{4\, H}$$

The soil can act as a filter and in some cases may amplify the motion of an earthquake producing more damages. The soft soils are the responsible of the amplification. In particular, if the resonance frequency of the soil is the same of the resonance frequency of the building, when there is an earthquake, the amplification is maximum and the effects are double; this phenomena is called resonance effect.

- Fundamental resonance frequency of a building: the measure is developed inside the building; if this one will be the same of the free field, there is the possibility to make some intervention on the structure to reduce the effects during an earthquake.

- Mean velocity of shear waves: there is the possibility to calculate $v_{s,30}$ knowing the depth of a known reflector. From this there is also the possibility to find the category of the soil as requested by NTC2018-

- Stratigraphy of the soil: it can reach until 700m of depth, but only the first 100m are more accurate. Each layer is considered as a single unit with certain characteristics and each one can be distinguished from the neighboring ones through an impedance contrast.

For the analysis it was used the "Tromino", this instrument is a triaxial single station seismometer where each velocimeter is defined by a frequency interval between 0.1 and 256 Hz. For the acquisition the instrument is leaved on the topographic surface, near the scene area and recorded the micro-tremors for 10 minutes. (*Figure 2.23*). The acquisition is done in the ground because in this way there is a better coupling between the soil and the instrument, otherwise there could be some errors on the frequency curve.



*Figure 2.23 - Instrument used for HVSR investigation*

## 2.4.1 Results

From the results there is the possibility find the depth of the bedrock and this corresponds to the peak value in the graph. In *Figure 2.24* is possible to see the presence of a HVSR peak around 65 Hz. No relevant impedance contrast is detectable. The very high frequency one is related to the very shallow subsoil cover. This is mainly due to the urban noisy environment and to the presence of a gradually increase of seismic velocity in depth, without relevant impedance contrasts.
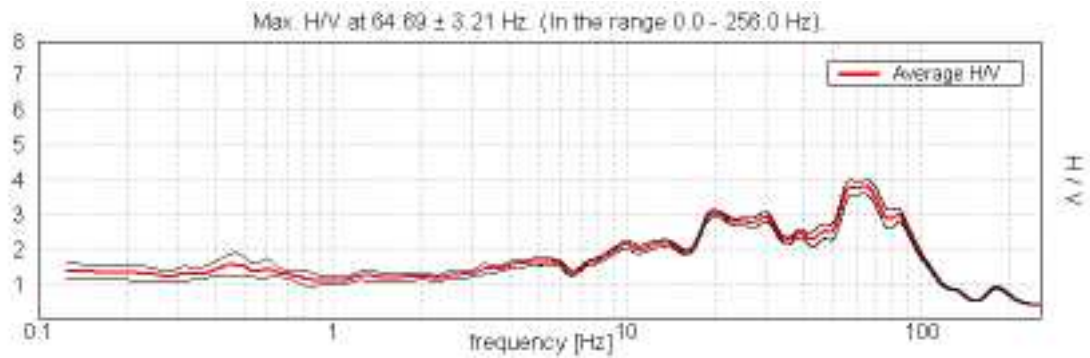


*Figure 2.24* - *H/V spectra at Roman Theater*

# *LOCAL SEISMIC RESPONSE*

To understand the seismic action at the level of the foundation, the local seismic response analysis is used. This type of analysis is carried out because in some cases the soil may modify and amplify the seismic motion produced by an earthquake. The velocity of the seismic waves depends on the elastic characteristics of the material and these, during their propagation path from the epicenter to the site, could be modified in terms of duration, amplitude and frequency. These characteristics must be quantified, thus a local seismic response analysis must be performed. This is a numerical analysis that submits different sections of the site to an earthquake placed at the base, to find the response of the area and possible amplifications of the seismic motion.

## 3.1 Amplification effects

The amplification of the seismic input is produced by the site effects. These are due to the lithological and morphological conditions. About the first one, this refers to the type of soil that characterized the site. The second one depends on the topography, in particular on the presence of slope, valley and cliff.

### 3.1.1 Lithological conditions

The type of soil could produce modifications on the seismic action. To understand if there is an amplification of the seismic input there is the possibility to calculate the transfer function. This is the spectral ratio between the motion at the basement and the motion at the ground surface (*Figure 3.1*):

$$F(f) = \frac{g(f)}{f(f)}$$

If $g(f) > f(f)$ means there is an amplification of the seismic motion. The transfer function is used to retrieve the amplification factor that is given by the modulus of the previous one:

$$Amplification\ factor = |F(f)|$$
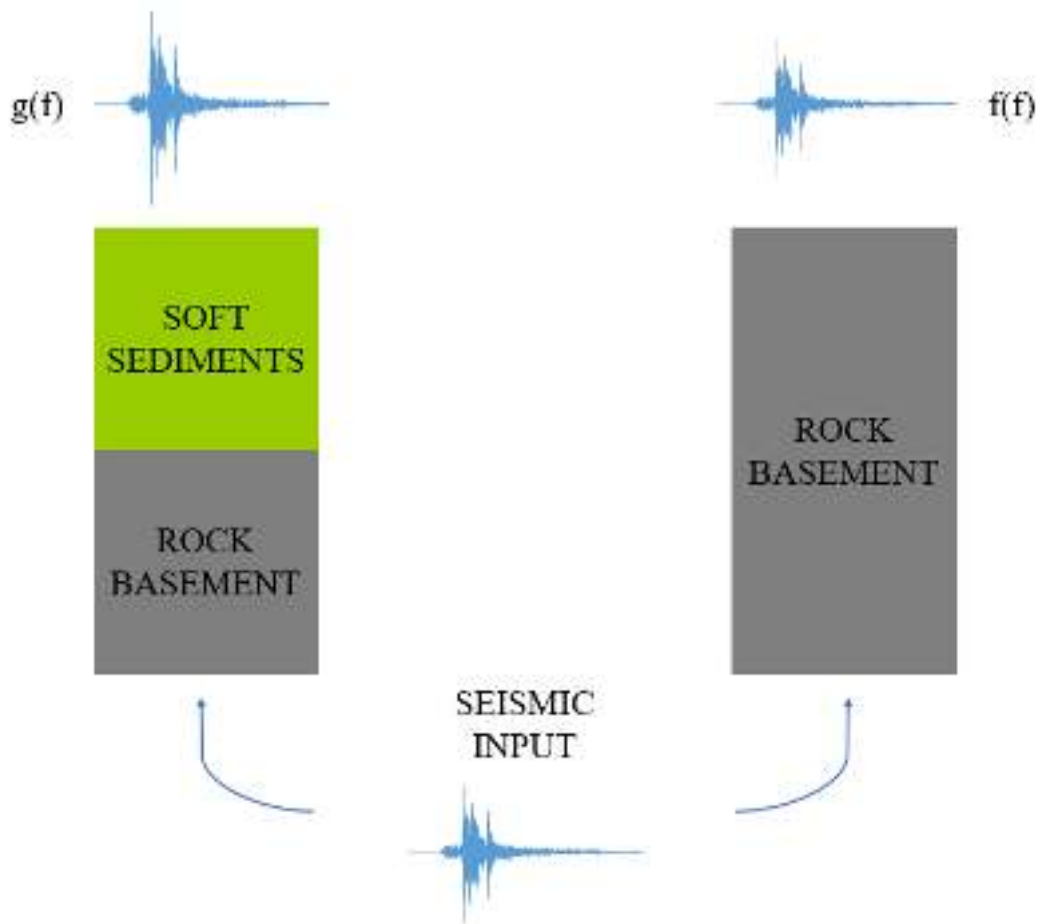
*Figure 3.1 - Output of the seismic motion in two different cases: in the right part the soil is only rock and the seismic action is not subjected to an amplification; in the left part above the rock there is soft soil that produces an amplification of the seismic input and the acceleration recorded at the surface is greater than the produced one.*

It was observed that if the soil is made only by rock there is an attenuation with the distance, so there are no modifications; otherwise, with the presence of soft soils the energy of the earthquake is modified and amplified. This amplification is due to conservation of energy, because are slower soil and improve the seismic acceleration.

To identify the type of soil that characterize the site of interest, the NTC2018, that are the construction technical standards published in 2018, denote 5 categories of soil that are reported in *Table 3.1*.

*Table 3.1 - Soil types from NTC2018*

| Category | Description |
|:---:|:---|
| A | Outcropping rock masses or very rigid soils characterized by shear wave velocity values higher than 800 m/s, possibly including on the surface soils with poorer mechanical characteristics with a maximum thickness of 3 m |
| B | Soft rocks and deposits of very dense coarse-grained soils or very consistent fine-grained soils, characterized by an improvement of the mechanical properties with depth and by equivalent velocity values between 360 m/s and 800 m/s |
| C | Deposits of medium-densified coarse-grained soils or medium-heavy fine-grained soils with substrate depths greater than 30 m, characterized by an improvement in mechanical properties with depth and by equivalent velocity values between 180 m/s and 360 m/s |
| D | Deposits of poorly densified coarse-grained soils or poorly consistent fine-grained soils, with substrate depths greater than 30 m, characterized by an improvement of the mechanical properties with depth and by equivalent velocity values between 100 and 180 m/s |
| E | Grounds with characteristics and equivalent speed values attributable to those defined for categories C or D, with substrate depth not exceeding 30 m. |

### 3.1.2 Topographic conditions

The topographic effects are less important than the lithological ones. These occur due to the constructive interference between the reflected waves and the boundaries effects. This type of effect can be significant if the dimensions are in the same order of the seismic wavelength.

$$2L = \lambda$$

where L is the half of the width of the topography and λ is the wavelength of the seismic wave. This means that bigger is the slope and bigger is the amplification. This problem could be caused also by the presence of valley. In this case happen that the energy is trapped in the valley and produces an amplification due to the interference between the waves. The effects of these depend on their geometry and the contrast between $v_1$ and $v_2$ (*Figure 3.2*). For this type of topography there is the possibility to calculate the shaper ratio:

$$shape\ ratio = \frac{H}{L}$$

where H is the depth of the valley and L is the length. Greater is the shape ratio and greater is the contrast between the two velocities. A higher contrast means that also the amplification will be higher and this happen in the case of deep valley.
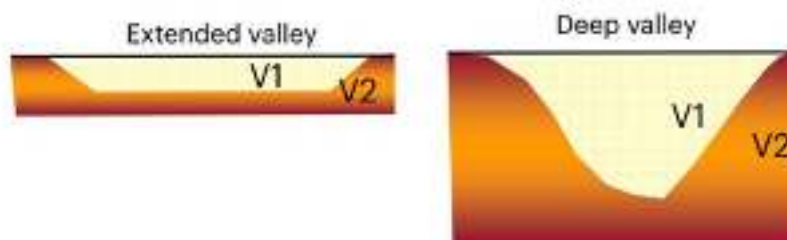


*Figure 3.2 – Different types of valleys: the extended valley is characterized by a low shape ratio. The deep valley has a great depth and these are morphological conditions that produces an amplification of the seismic input*

The NTC2018 also proposed a classification for the different type of topography and these are reported in *Table 3.2*.

*Table 3.2 - Topographic category form NTC2018*

| Category | Description |
|:---:|:---|
| **T1** | Flat surface, slopes and isolated reliefs with average inclination i ≤ 15° |
| **T2** | Slopes with an average inclination i > 15° |
| **T3** | Reliefs with crest width much smaller than at the base and average inclination 15° ≤ i ≤ 30° |
| **T4** | Reliefs with crest width much smaller than at the base and average inclination i > 30° |

## 3.2 Seismic local response analysis of Roman Theater area

For this analysis a 2D model is implemented and there are a series of steps to follow: geometry definition, dynamic characterization of the soils involved, choice of one or more input earthquakes and the use of a calculation code. The output is the description of the surface motion in the form of an accelerogram, from which an elastic response spectrum can be extrapolated. An equivalent linear model is used, which "*[...] consist in solving a no linear problem through complete linear analyses in which, at the end of each iteration, the stiffness and damping parameters are updated, which are depending on the state of deformation of the ground [...]*" [Nori et al, 2024]. Indeed, an important aspect is to consider the deformation of the soil, because during an earthquake the stress applied is high and produces a permanent deformation of it. In *Figure 3.3* is represent the relation between the stress and strain of a soil during an earthquake.
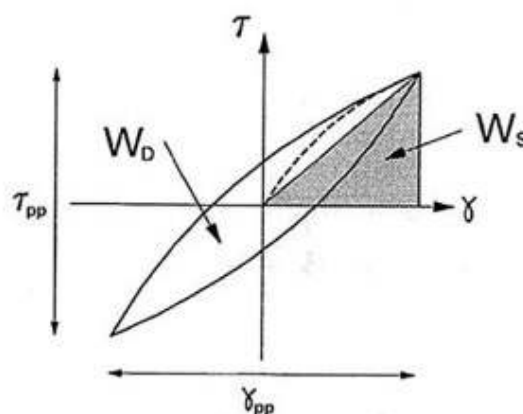


**Figure 3.3** – *Diagram shear stress-strain in relation to the damping. $W_D$ is the dissipated energy per cycle, $W_S$ is the elastic energy (maximum deformation energy)*

This behavior is due to the dissipative character of the soil, that means it loose energy during the process. The two parameters that have to be considered for each layer are the shear modulus G, correlated to $v_s$ and the density, and the damping D that represents the ability of the soil to dissipate the energy. These are given by:

$$G = \frac{\tau_{pp}}{\gamma_{pp}}$$

$$D = \frac{W_D}{4\pi W_S}$$

G and D varying in function of the deformation, in particular G decreases with the increase of the deformation and D increases with the increase of the deformation (*Figure 3.4* and *3.5*).



**Figure 3.4** - *Variation of G with the deformation for a sandy soil*
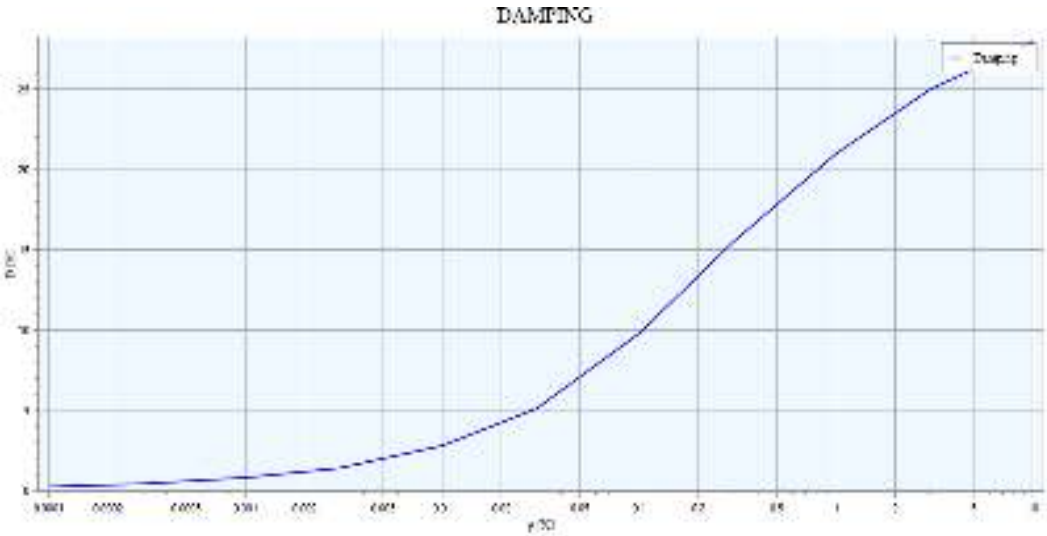


**Figure 3.5** - *Variation of D with the deformation for a sandy soil*

### 3.2.1 LSR2D software

For this analysis the software LSR2D is used. This performs a numerical analysis using a section of the site. Each layer is represented by a polygon characterized by a certain density, $v_s$, damping and shear modulus. This is stressed through a series of waves at the base of the section and it is observed what happens in the different control points, in order to have a comparison between the base and the points on the surface. During the simulation, it is necessary to pay attention to the lateral extremities because in correspondence with these there could be some reflection of the waves. To solve the problem, some free-field will be add.

For this site was proposed a section along the scene area of the Roman Theater (*Figure 3.6*).
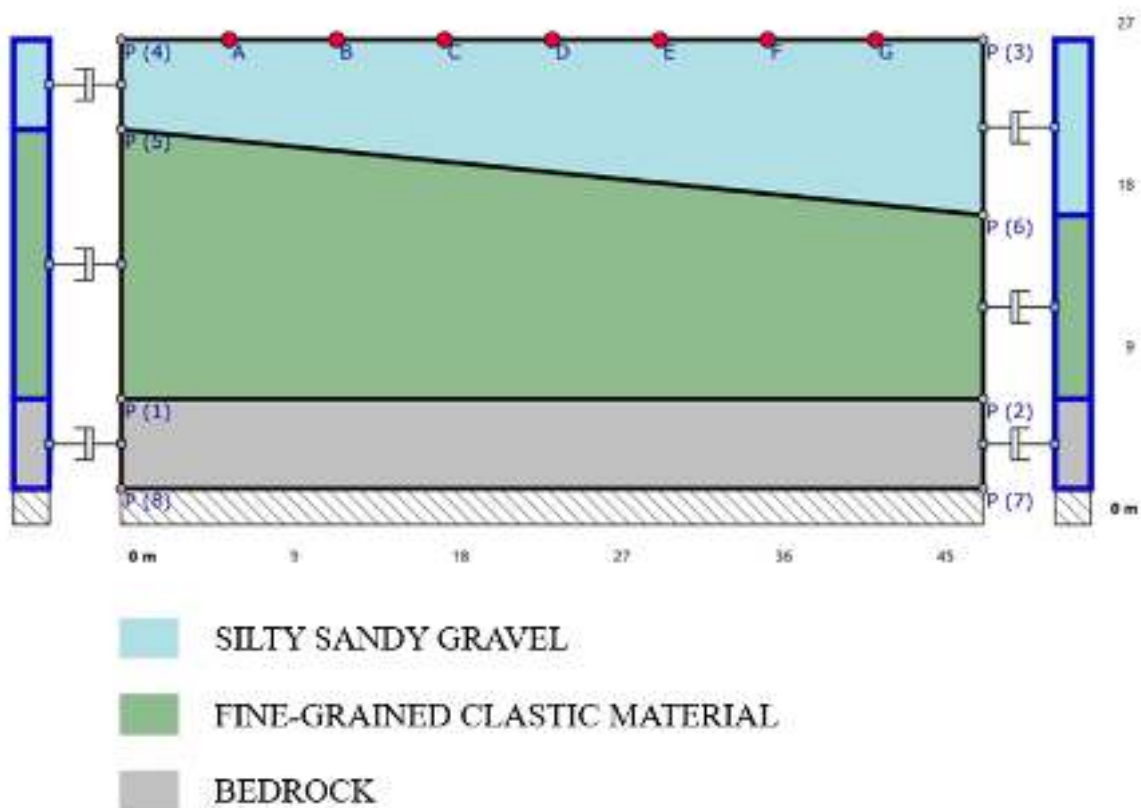


*Figure 3.6 - Section on the software LSR2D of the scene area if the Roman Theater*

The section is characterized by 3 different layers: the silty sandy gravel, the fine-grained material and the bedrock, where the characteristics are reported in *Table 2.2*. The red dots represent the control point from which you get the outputs.

As already discussed in chapter 1, the study area is situated above an active fault that is the Adige Plain. This could produce high intensity earthquake. In this study two different analyses were performed. The first one follows the regulations for the seismic local response: the input is a set of seven accelerogram. The second one consists in a simulation of the worst case: the

input is an earthquake with the same characteristics of the 1117 ones (that for simplicity, in the analyses, it will be called 1117 earthquake from now on). It represents the strongest seismic event recorded in this area.

### 3.2.2 Results

In this analysis are taken in consideration only the results of point G (*Figure 3.6*), this because is the point with the greatest thickness of the first layer and produces the most dangerous results. From the first analysis seven accelerograms are obtained. From these the corresponding seismic response spectra and the average response spectra can be extrapolated (*Figure 3.7*).
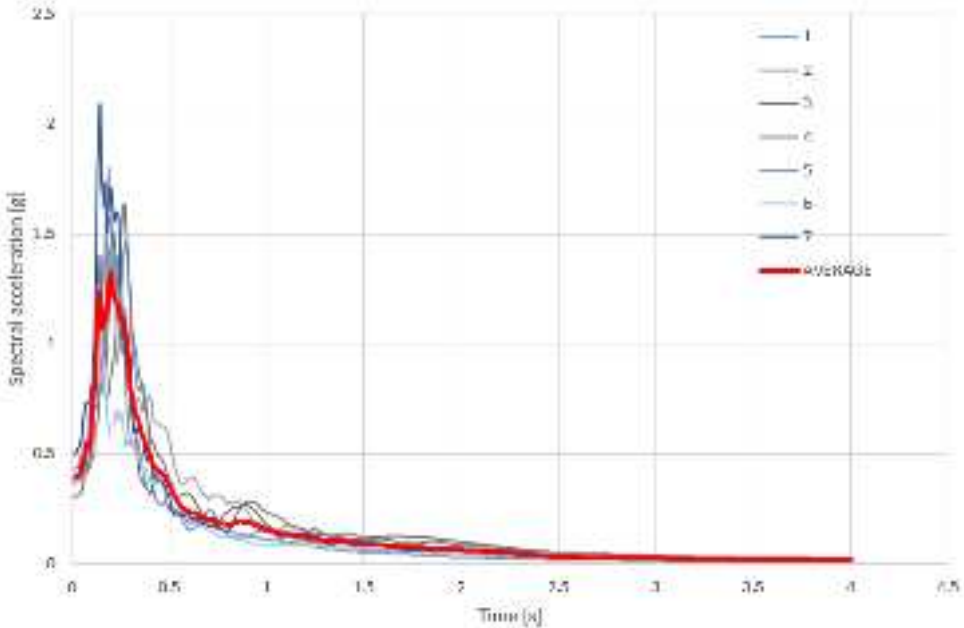


**Figure 3.7** – *Response spectra of the analysis with the set of accelerograms. The red one is the average*

The same procedure can be done for the earthquake of 1117 (*Figure 3.8*).
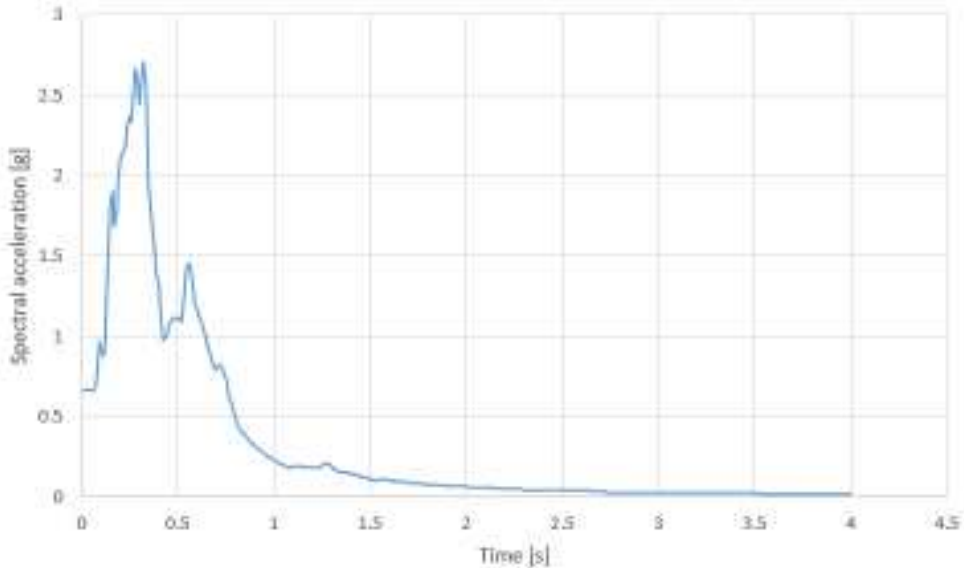


**Figure 3.8** - *Response spectra obtained from the local response analysis in the case of the earthquake of 1117*

Comparing the two resultant spectra (*Figure 3.9*), it is possible to see that the earthquake of 1117 reaches a higher spectral acceleration than the seismic response analysis, indeed the first is about 2.7g otherwise for the other reaches 1.3g.
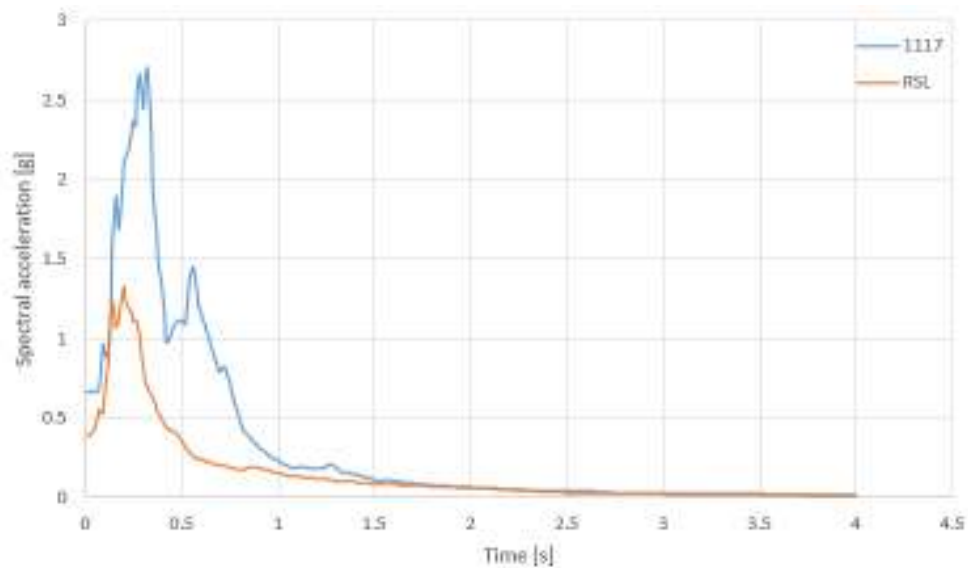


***Figure 3.9*** - *Comparison between the response spectra of the two previous analyses. The orange one is the average of the seven spectra; the blue one refers to the earthquake of 1117*

Subsequently, the spectra are transformed in spectra with a standard shape, according to the technical standards for constructions. There are different methods for the normalization:

- the total normalization, that does not follow a normative reference and is used to obtain a spectrum that contains the one resulting from the LSR
- the normalization according to Order No. 55 of 24th April 2018, *"[...] allows to transform the response spectrum, result of numerical simulations in the context of studies of MS3, in a spectrum with standard form (according to current technical standards for construction), consisting of a branch with constant acceleration, a branch in which the acceleration decreases with 1/T and, therefore, at constant speed. At the end of the procedure will also be available all the parameters for the design and verification of constructions [...]"* [Order No 55 of 24th April 2018].

Few parameters that can be calculated with the normalization are the maximum acceleration and the soil amplification factor. The maximum acceleration $a_{max}$ represents the maximum acceleration recorded at the surface and is different for each analysis. The soil amplification factor S, is another important parameter and is given by the stratigraphic coefficient $S_S$ and the topographic coefficient $S_T$. For this site S is equal to 2.121. (*Figure 3.10* and *3.11*).
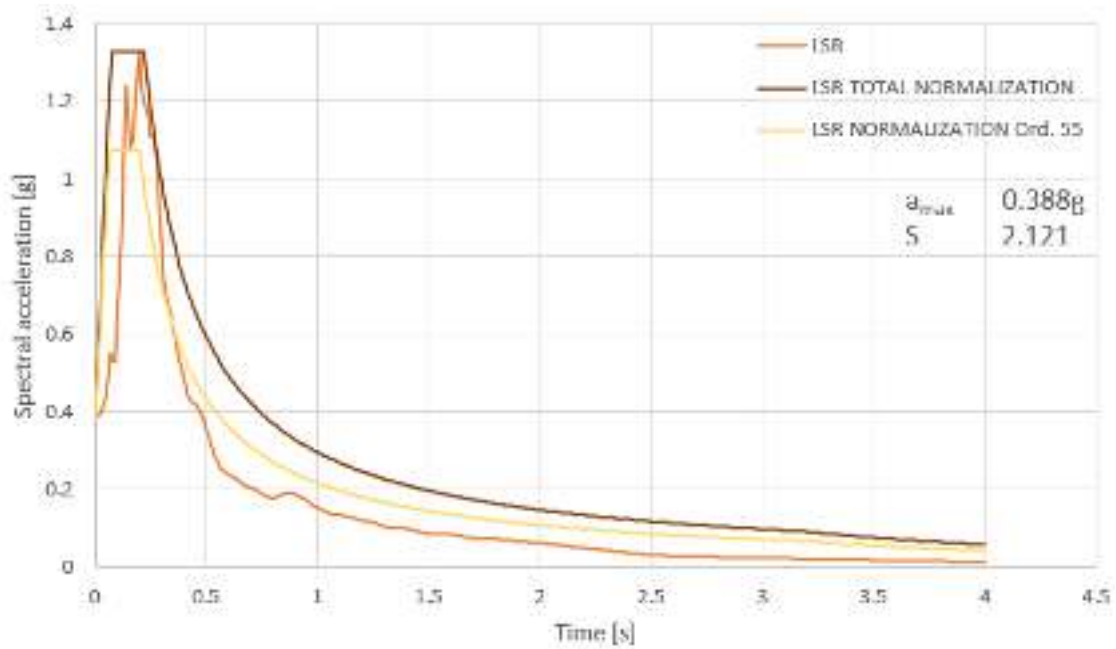
***Figure 3.10*** *- Response spectra and its normalization for the average of the seven response spectra. The orange is the response spectrum obtained from the local response analysis, the brown is the normalized spectra using the total normalization, the yellow is the response spectra normalized following the Order No. 55. $a_{max}$ is the maximum acceleration recorded at the surface, S is the soil amplification factor for the site*
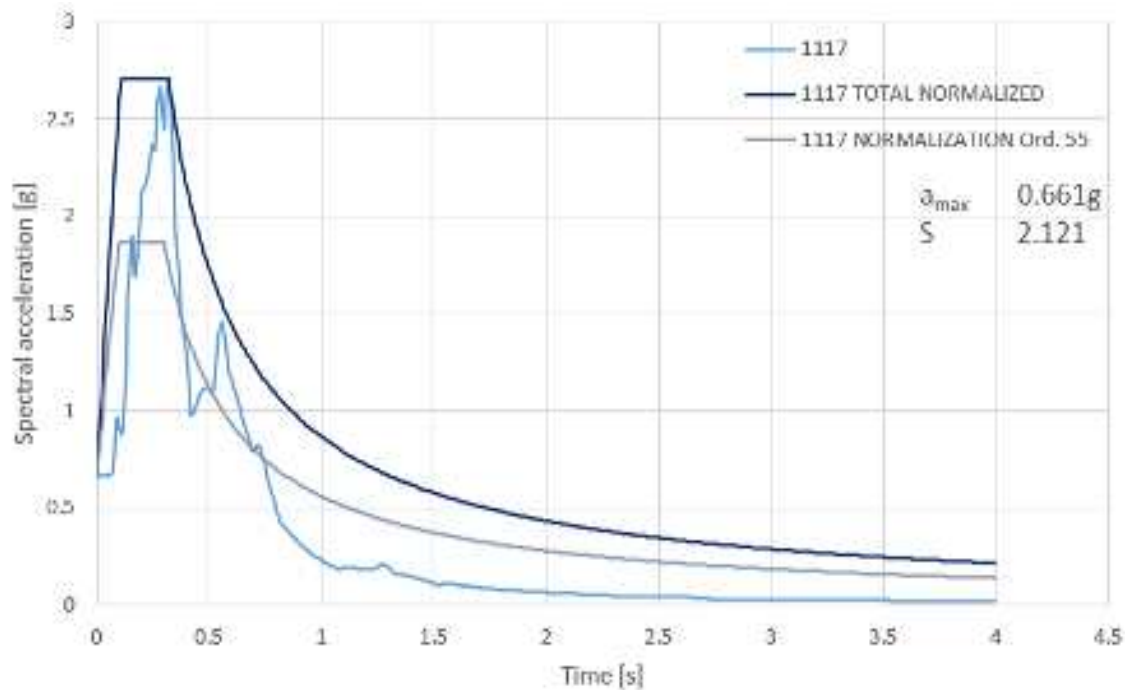


***Figure 3.11*** *- Response spectra and its normalization for the earthquake of 1117. The blue is the response spectrum obtained from the local response analysis, the dark blue is the normalized spectra using the total normalization, the grey is the response spectra normalized following the Order No. 55. $a_{max}$ is the maximum acceleration recorded at the surface, S is the soil amplification factor for the site*

Looking at accelerograms, it is clearly that the event of 1117 on the surface have the highest acceleration. Indeed, it turns out that the Verona's earthquake has an acceleration higher than 58% (*Figure 3.12*).

42

**AVERAGE LOCAL SEISMIC RESPONSE ACCELEROGRAM**

**1117 LOCAL SEISMIC RESPONSE ACCELEROGRAM**

**COMPARISON BETWEEN ACCELEROGRAMS**
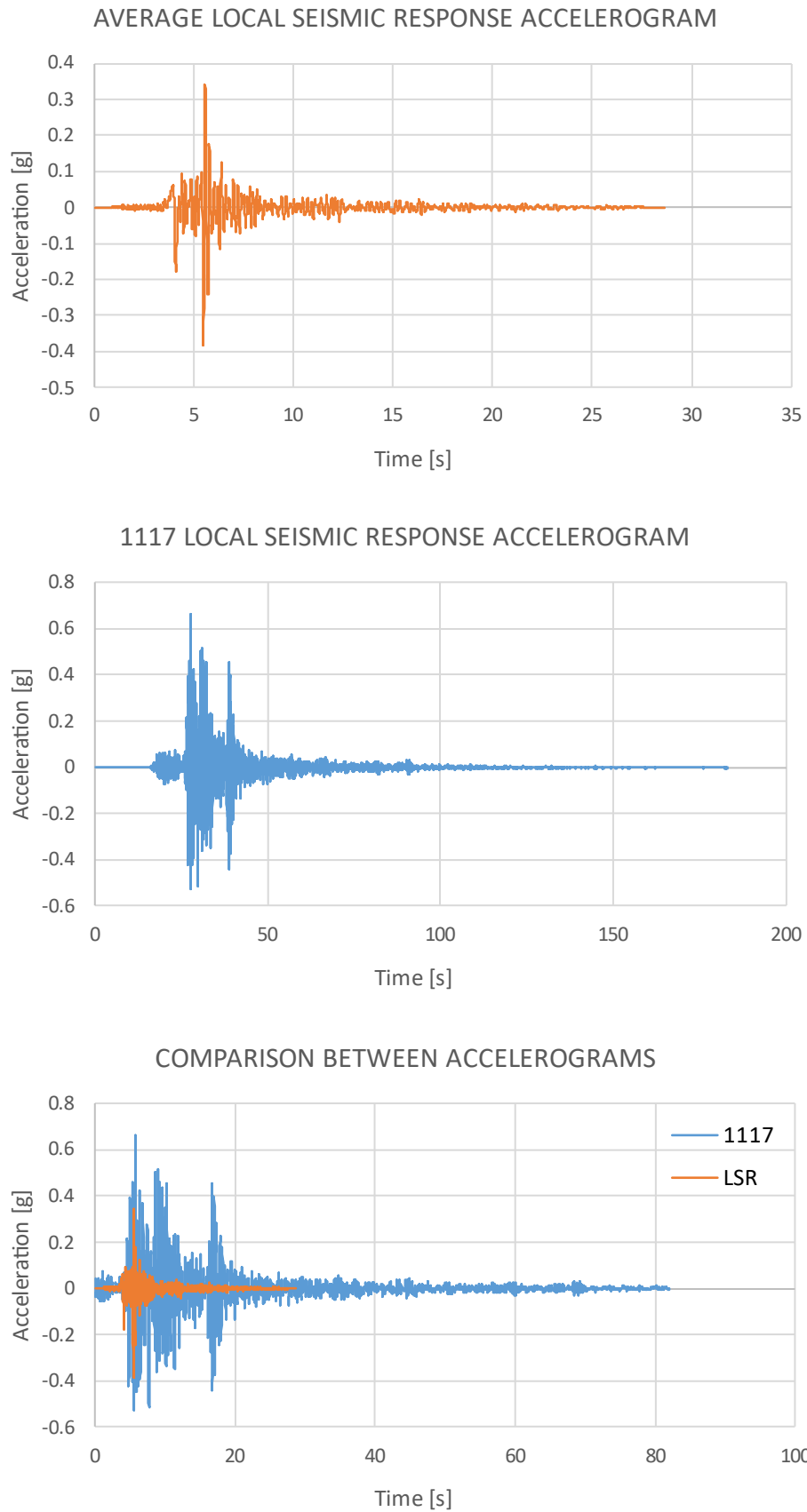
***Figure 3.12*** *- Accelerograms obtained from the two analyses. The first one represents the mean accelerogram recorded at the surface in the case of local seismic response analysis with the set of accelerograms. The second one is the resultants accelerogram for 1117 earthquake. The third one is the comparison between the two accelerograms, the blue one has been cut in the first part in order to have the coincidence of the peaks*

43

An interesting comparison is between the spectra obtained from the two analyses and the response spectrum of the seismic action for the generic site (*Figure 3.13*). The Roman Theater area is characterized by a soil type E and a topographic category T1 (*Table 3.1 – 3.2*).



**Figure 3.13** - *Comparison between the normalized spectra (following the Order No. 55) of the earthquake of 1117 (blue), the set of accelerogram (orange) and site with soil E and topography T1 (green)*

The seismic local response analysis is defined as a rigorous approach, because through an accurate analysis performs the different parameters that are fundamental to define the response spectra. Otherwise, the simple approach consists only in the estimation of the spectra considering only the soil and topographic category defined by NTC2018. As shown in *Figure 3.14*, it can be stated that the local seismic response analysis is stricter than the other method. Indeed, if the spectrum given by the standards and the spectrum obtained from the local response analysis with the set accelerogram are considered, it is possible to say that they have a different shape. The first thing to observe is the maximum acceleration: the Italian seismic code claims that in soil of type E the $a_g$ is 0.183, but as demonstrated through the LSR analysis the $a_g$ is 0.38. In the worst case, the acceleration reaches 0.66. Then 0.4s it can be observed that the LSR spectrum is below that provided by the standards; this means that for periods higher than 0.4, the regulations expect ground acceleration greater than those obtained from the analysis. Despite this, it can still be state that the simplified approach is in any case less rigorous than the seismic response analysis. About the earthquake of 1117, its spectrum is clearly above that of standards since the latter does not take exceptional events into consideration. Regarding the accelerations, a further comparison can be done looking at the

accelerograms: the two obtained from the LSR analysis and the one obtained from the average of a set of seven accelerograms spectral compatible with the elastic response spectrum relating to the ground E (*Figure 3.14*). As already said, the regulation provides reduced accelerations compared to those that occur in reality.
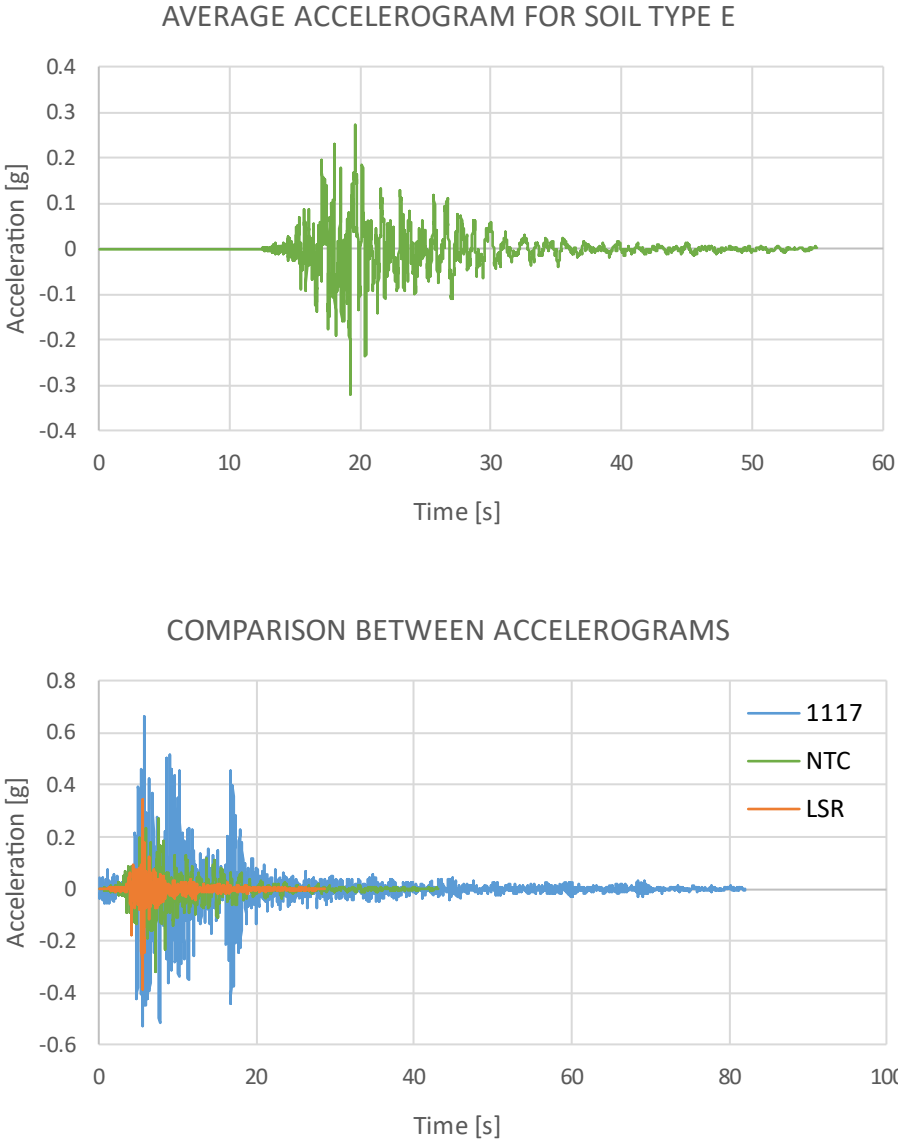


*Figure 3.14* - *Average accelerogram of a set of seven accelerogram spectral compatible to a soil type E. Below the comparison between the three accelerograms: the one provided by the standards (green) and the two obtained by the local response analysis (blue for the 1117 earthquake and orange for the set of accelerograms). The blue and the green ones have been cut in the first part in order to have the coincidence of the peaks*

Another observation that could be done is about the type of soil that was considered. The soil E is a soil with intermediate characteristics between soil C and soil D. If the site had different soil, the response spectrum would have been different (*Figure 3.15*).
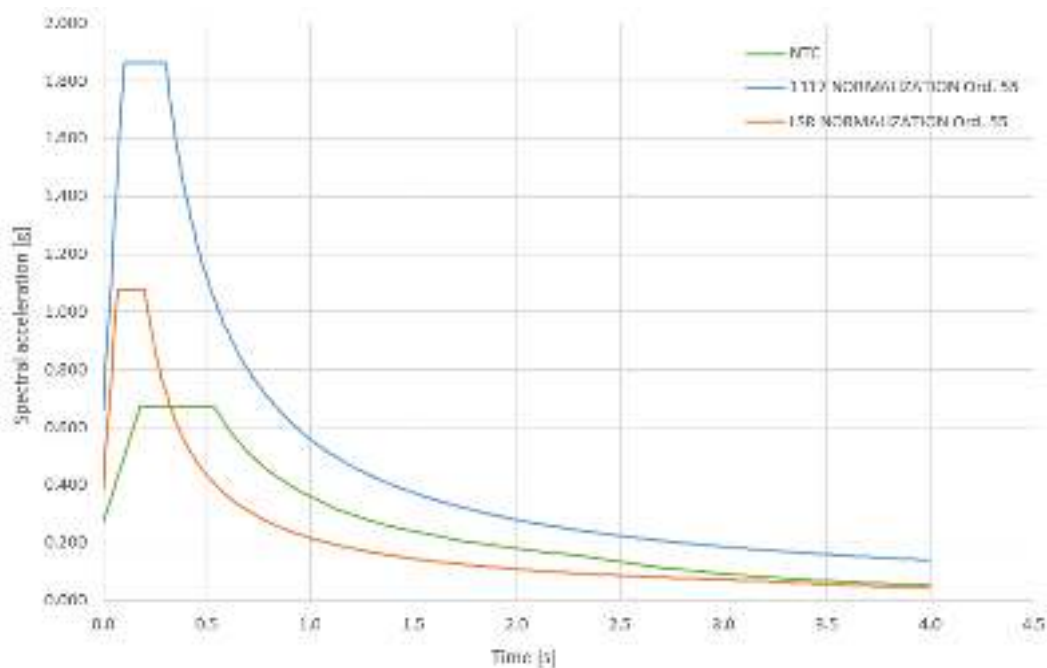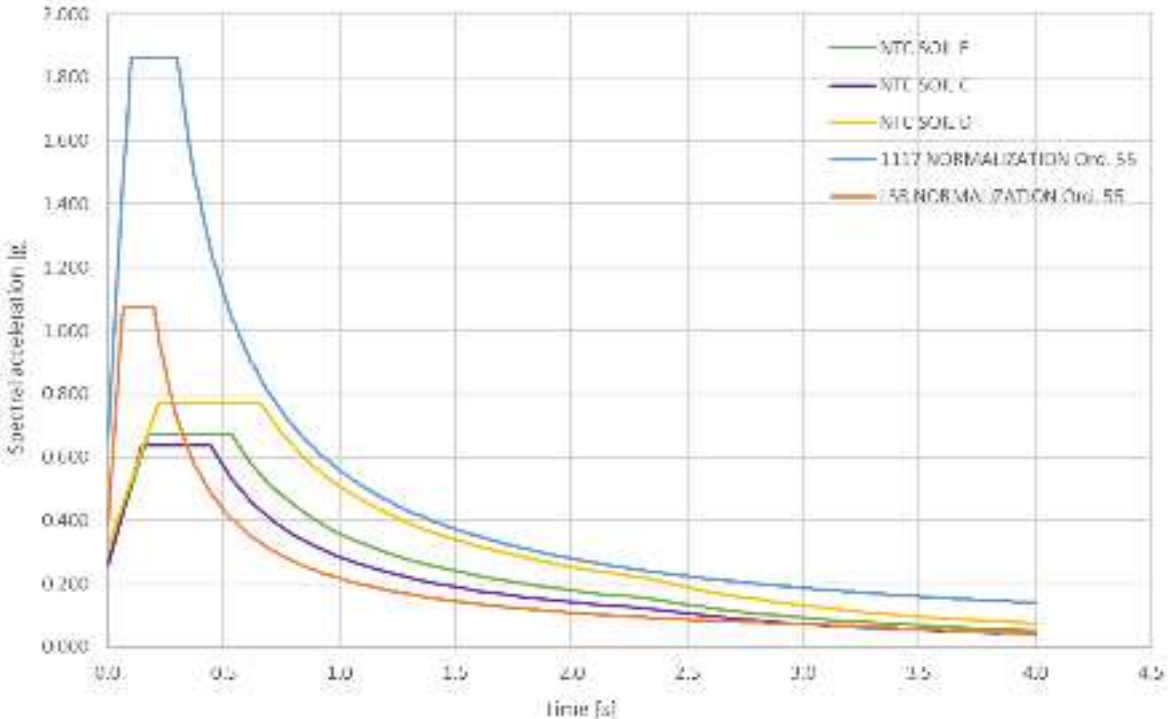


***Figure 3.15*** – *Comparison between the normalized spectra (following the Order No. 55) of the earthquake of 1117 (blue), the set of accelerogram (orange), site with soil E and topography T1 (green), site with soil C and topography T1 (purple), site with soil D and topography T1 (yellow)*

Indeed, if the spectrum of soil D is observed, this is characterized by a greater maximum acceleration than soil C and E, and already around 0.3s it has spectral accelerations higher than those obtained from the LSR analysis.

# *KINEMATIC ANALYSIS*

The damage and collapse checks can be done through the analysis of the local mechanism. This is a kinematic approach and "*[…] it is based on the choice of the collapse mechanism and the evaluation of the horizontal action […].*" [Vinci, 2019].

This method evaluates the local mechanism that are the most significant for the structure. For the application of the analysis, it is assumed that the tensile strength of the masonry is zero, that there is no sliding between the blocks and that the compressive strength of the masonry is infinite. The fundamental step in this analysis is to find the horizontal load multiplier $\alpha_0$, also defined as mechanism activation multiplier, that produces the activation of the mechanism. This analysis is made on the scene area of the Roman Theater. Two different kinematic analysis will carry out: one with the results obtained from the seismic local response analysis and one with the values of the NTC2018.

## 4.1 Theory of calculation technique

In this analysis the linear kinematic approach is implemented. In this case, will be analyzed singularly each wall of the scene area of the Roman Theater (*Figure 4.3*).
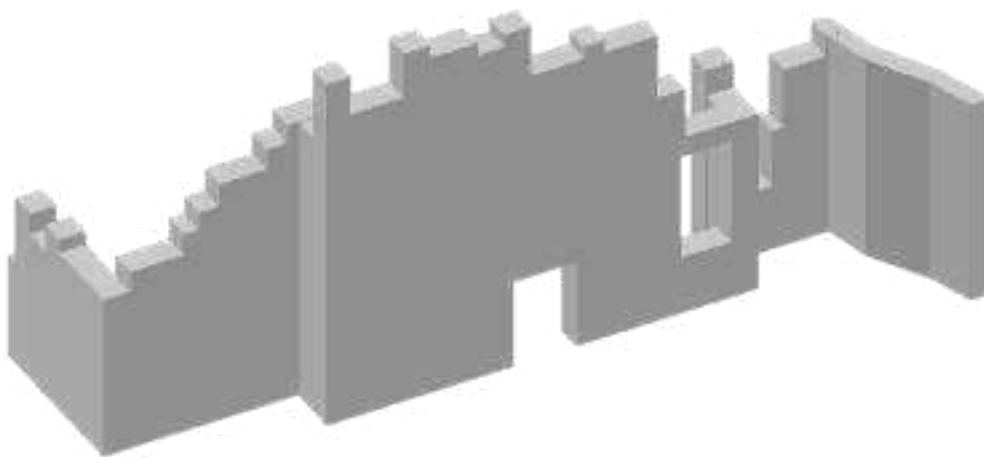


*Figure 4.3 - Scene area of the Roman Theater*

"*The analyzed portion of the structure is considered labile and each element of which it is composed is free to rotate around a point called kinematic hinge*" [Vinci, 2019]. The first step consists in the individuation of a kinematic chain, namely a portion of the structure that is considered independent. Each system is subjected only to the vertical force, due to weight of

the wall (W) and to the horizontal force that is generated under the seismic effect of the weight of the wall (*Figure 4.4*).
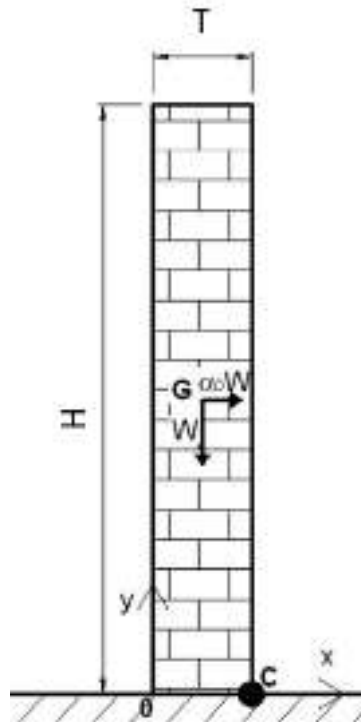


**Figure 4.4** - *Scheme of the wall*

From *Figure 4.4* is possible to see:

C: position of the hinge

H: height of the wall

T: thickness of the wall

G: center of gravity of the wall

W: weight of the wall, that is given by:

$$W = \gamma\, H\, T\, L$$

where $\gamma$ is the specific weight of masonry, that is equal to 16 kN/m³ and L is the length of the wall. For the linear calculation the horizontal load multiplier needs to be found. This can be obtained through the Principle of Virtual Works that says: "*necessary and sufficient condition for any material system to be in equilibrium is that the sum of all the forces acting on the system, multiplied by an infinitesimal displacement compatible with the constraints, is zero.*" [Vinci, 2019]

$$L_{int} = L_{ext}$$

In this case, the out of plane mechanism can be interpreted with simple rotation; in this way is possible to reduce the principle to a rotational equilibrium around the hinge that can be defined as:

$$M_{stabilizing} = M_{overturning}$$

The stabilizing momentum is given by:

$$M_{stabilizing} = W * \left(\frac{T}{2} - a\right)$$

where $a$ is the offset of the hinge. Indeed, for a more realistic simulation of the structural behavior, the location of the rotation hinge is assumed to be set back from the edge of the wall. This assumption is considered because, as the rotation angles become larger, the load is concentrated on a small portion of the wall, thus, the stress on the masonry increase until the maximum resistance of the material is reached, generating a fracture of the wall edge. This retreat must be considered because the distance between the rotational point and the stabilizing force decreases (*Figure 4.5*).
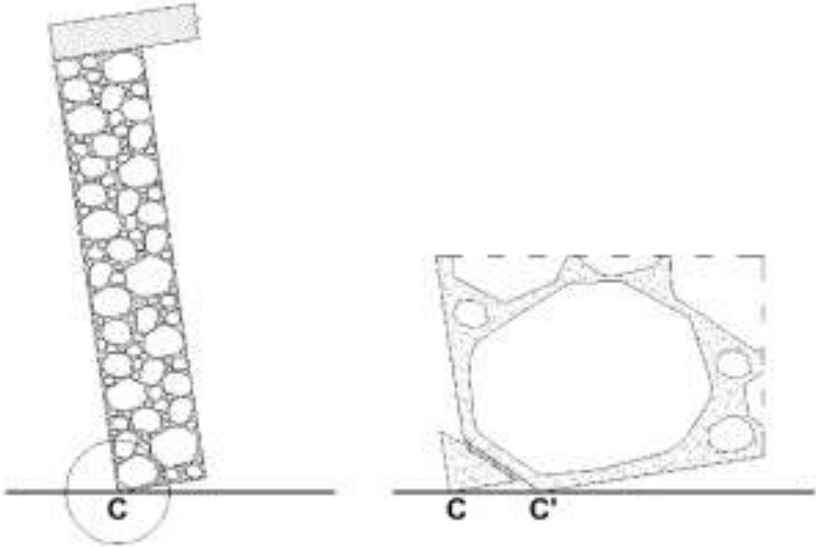


*Figure 4.5 - Scheme of the hinge retreat*

The retreat is given by:

$$a = \frac{2\,W}{3\,L\,f_d}$$

where $f_d$ is the limit normal stress and is equal to:

$$f_d = \frac{f_k}{\gamma_m \, FC}$$

$f_k$ is the characteristics compressive strength of the masonry equal to 2600 kN/m$^2$

$\gamma_m$ is the masonry safety factor equal to 2

FC is the confidence factor equal to 1.2

For the analysis the limit normal stress is:

$$f_d = 1083.33 \, kN/m^2$$

The overturning moment is given by:

$$M_{overturning} = W \, H_G$$

The horizontal load multiplier is obtained between the ratio of stabilizing and overturning momentum.

$$\alpha_0 = \frac{\frac{T}{2} - a}{H_G}$$

From $\alpha_0$ is possible to retrieve $a_0^*$ that is the spectral seismic acceleration of mechanism activation:

$$a_0 * = \frac{\alpha_0}{e * FC}$$

$$e * = \frac{M * g}{W}$$

$$M * = \frac{(W \, \delta_{x,w})^2}{g \, (W \, \delta_{x,w}{}^2)}$$

M* is the participating mass

$\delta_{x,w}$ is the horizontal virtual displacement of the point of application of the weight

The safety check was carried out for the life limit state (SLV). For this limit state is required to find $a_0^*$ from which is possible to retrieve the capacity acceleration. The check consists in the ratio between the capacity acceleration and the request acceleration that is equal to 0.183g. If the ratio is bigger than 100% it is verified, otherwise not.

## 4.2 Kinematic analysis of the scene area

In this part will be showed all the results obtained from the kinematic analysis for each wall of the scene area of the Roman Theater. This area is characterized by different blocks with a regular shape. Although some parts are composed by different materials, for the analysis is considered that each block is made only by masonry. The constants that will be used for the analysis are reported in *Table 4.1*.

*Table 4.1 - Constants used for the kinematic analysis*

| | | |
|---|---|---|
| Acceleration at bedrock | $a_g$ [g] | 0.183 |
| Soil amplification factor for RSL | $S_{RSL}$ | 1.742 |
| Soil amplification factor for NTC | $S_{NTC2018}$ | 1.506 |
| Compressive strength | $f_k$ [kN/m$^2$] | 2600 |
| Masonry safety factor | $\gamma_m$ | 2 |
| Specific weight | Ps [kN/m$^3$] | 16 |
| Confidence factor | FC | 1.2 |
| Limit normal stress | $f_d$ [kN/m$^2$] | 1083.33 |
| Structural factor | q | 2 |
| Acceleration of gravity | g [m/s$^2$] | 9.81 |

**SCENE A**
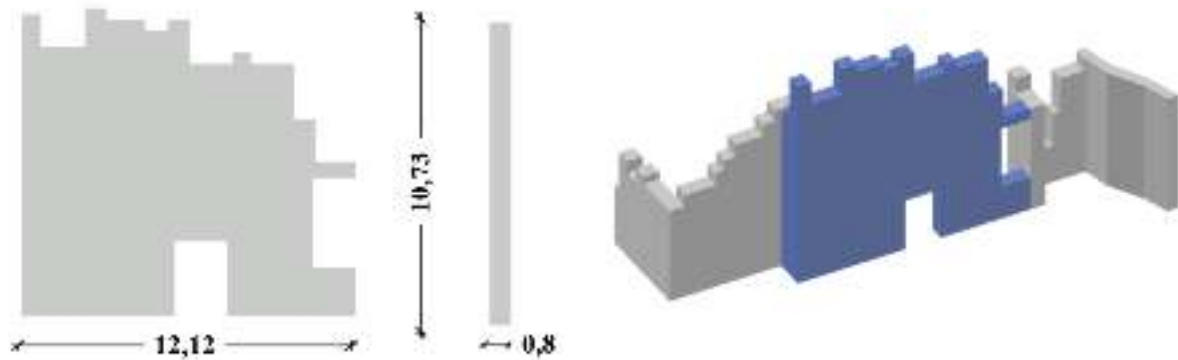


*Figure 4.6 - Dimensions of the wall A of the scene area*

H = 10.73 m                                         $H_G$ = 5.03 m

T = 0.8 m                                           $T_G$ = 0.4 m

L = 12.12 m

## Load multiplier

| W (kN) | a (m) | $\frac{T}{2} - a$ (m) | $M_S$ (kNm) | $M_T$ (kNm) | $\alpha_0$ |
|--------|-------|-----------------------|-------------|-------------|------------|
| 1314.15 | 0.067 | 0.333 | 437.97 | 6610.19 | 0.066 |

## RSL linear analysis

| M* (kg) | e* | $a_0^*$ (m/s²) | ag $_C$ (g) | ag $_D$ (g) | $\xi$ (%) |
|---------|-----|----------------|-------------|-------------|-----------|
| 133.961 | 1 | 0.110 | 0.031 | 0.183 | **28.45 %** |

## NTC2018 linear analysis

| M* (kg) | e* | $a_0^*$ (m/s²) | ag $_C$ (g) | ag $_D$ (g) | $\xi$ (%) |
|---------|-----|----------------|-------------|-------------|-----------|
| 133.961 | 1 | 0.110 | 0.073 | 0.183 | **40.07 %** |

**SCENE B**
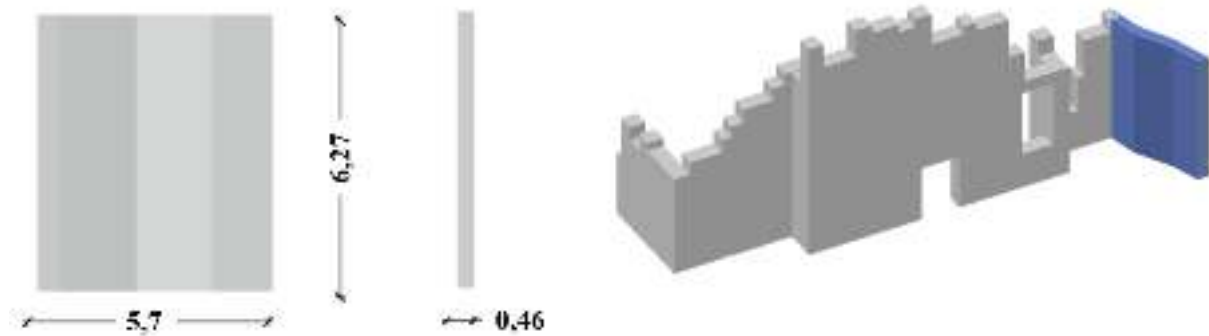


*Figure 4.7 - Dimensions of the wall B of the scene area*

H = 6.27 m                         $H_G$ = 3.13 m

T = 0.46 m                         $T_G$ = 0.23 m

L = 5.7 m

## Load multiplier

| W (kN) | a (m) | $\frac{T}{2} - a$ (m) | $M_S$ (kNm) | $M_T$ (kNm) | $\alpha_0$ |
|--------|-------|------------------------|-------------|-------------|-----------|
| 263.04 | 0.028 | 0.202 | 53.03 | 824.63 | 0.064 |

## RSL linear analysis

| M* (kg) | e* | $a_0$* (m/s²) | ag $_C$ (g) | ag $_D$ (g) | ξ (%) |
|---------|----|---------------|-------------|-------------|-------|
| 26.81 | 1 | 0.107 | 0.062 | 0.183 | **27.61 %** |

## NTC2018 linear analysis

| M* (kg) | e* | $a_0$* (m/s²) | ag $_C$ (g) | ag $_D$ (g) | ξ (%) |
|---------|----|---------------|-------------|-------------|-------|
| 26.81 | 1 | 0.107 | 0.071 | 0.183 | **38.89 %** |

**SCENE C**
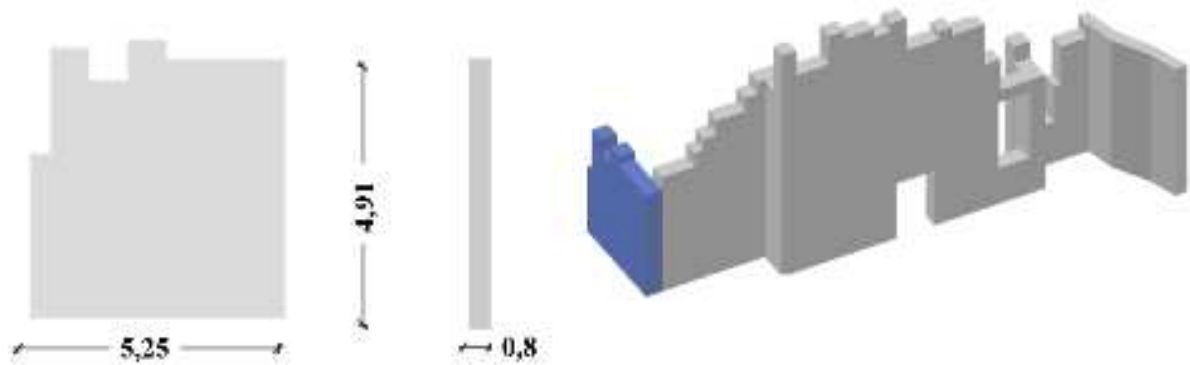


*Figure 4.8 - Dimensions of the wall C of the scene area*

H = 4.91 m $\qquad$ H$_G$ = 2.48 m

T = 0.8 m $\qquad$ T$_G$ = 0.4 m

L = 5.25 m

## Load multiplier

| W (kN) | a (m) | $\frac{T}{2}$ − a (m) | M$_S$ (kNm) | M$_T$ (kNm) | α$_0$ |
|---|---|---|---|---|---|
| 330.08 | 0.039 | 0.361 | 119.26 | 818.60 | 0.146 |

## RSL linear analysis

| M* (kg) | e* | a$_0$* (m/s²) | ag $_C$ (g) | ag $_D$ (g) | ξ (%) |
|---|---|---|---|---|---|
| 33.647 | 1 | 0.243 | 0.139 | 0.183 | **62.56 %** |

## NTC2018 linear analysis

| M* (kg) | e* | a$_0$* (m/s²) | ag $_C$ (g) | ag $_D$ (g) | ξ (%) |
|---|---|---|---|---|---|
| 33.647 | 1 | 0.243 | 0.161 | 0.183 | **88.10 %** |

**SCENE D**
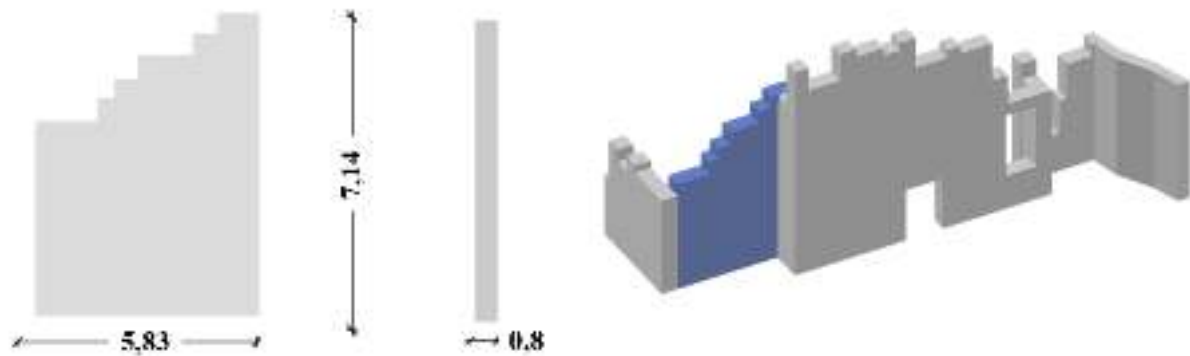


*Figure 4.9 - Dimensions of the wall D of the scene area*

H = 7.14 m                                    $H_G$ = 3.66 m

T = 0.8 m                                      $T_G$ = 0.4 m

L = 5.83 m

## Load multiplier

| W (kN) | a (m) | $\frac{T}{2} - a$ (m) | $M_S$ (kNm) | $M_T$ (kNm) | $\alpha_0$ |
|:---:|:---:|:---:|:---:|:---:|:---:|
| 533.44 | 0.056 | 0.344 | 183.34 | 1952.39 | 0.094 |

## RSL linear analysis

| $M^*$ (kg) | $e^*$ | $a_0^*$ (m/s²) | $ag_C$ (g) | $ag_D$ (g) | $\xi$ (%) |
|:---:|:---:|:---:|:---:|:---:|:---:|
| 54.377 | 1 | 0.157 | 0.090 | 0.183 | **40.32 %** |

## NTC2018 linear analysis

| $M^*$ (kg) | $e^*$ | $a_0^*$ (m/s²) | $ag_C$ (g) | $ag_D$ (g) | $\xi$ (%) |
|:---:|:---:|:---:|:---:|:---:|:---:|
| 54.377 | 1 | 0.157 | 0.104 | 0.183 | **56.79 %** |

55
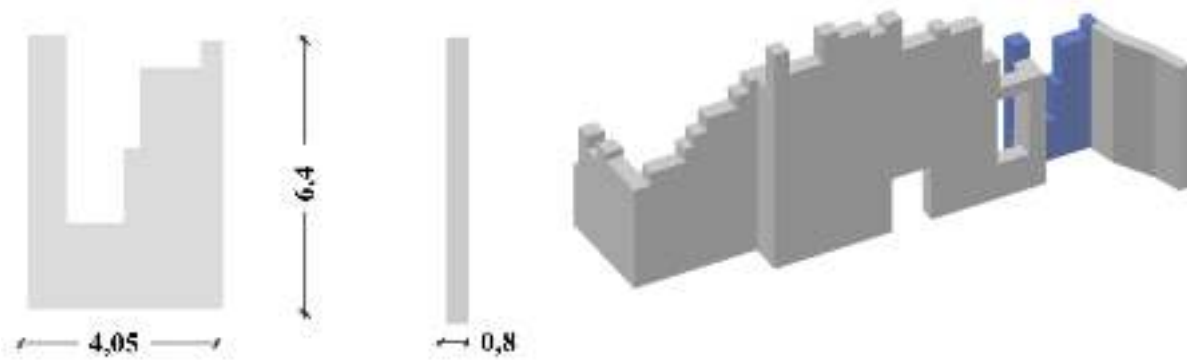
**SCENE E**



*Figure 4.10* - *Dimensions of the wall E of the scene area*

H = 6.4 m                                        $H_G$ = 2.67 m

T = 0.8 m                                        $T_G$ = 0.4 m

L = 4.05 m

## Load multiplier

| W (kN) | a (m) | $\frac{T}{2}$ − a (m) | $M_S$ (kNm) | $M_T$ (kNm) | $\alpha_0$ |
|:---:|:---:|:---:|:---:|:---:|:---:|
| 241.57 | 0.037 | 0.363 | 87.76 | 644.99 | 0.136 |

## RSL linear analysis

| M* (kg) | e* | $a_0$* (m/s²) | ag $_C$ (g) | ag $_D$ (g) | ξ (%) |
|:---:|:---:|:---:|:---:|:---:|:---:|
| 24.625 | 1 | 0.227 | 0.130 | 0.183 | **58.42 %** |

## NTC2018 linear analysis

| M* (kg) | e* | $a_0$* (m/s²) | ag $_C$ (g) | ag $_D$ (g) | ξ (%) |
|:---:|:---:|:---:|:---:|:---:|:---:|
| 24.625 | 1 | 0.227 | 0.151 | 0.183 | **82.28 %** |

## 4.3 Analysis of the results

An interesting aspect is to analyze the load multiplier coefficients; it is possible to represent these in a histogram in which each column represents the value of $\alpha_0$ for a single wall (*Figure 4.11*).
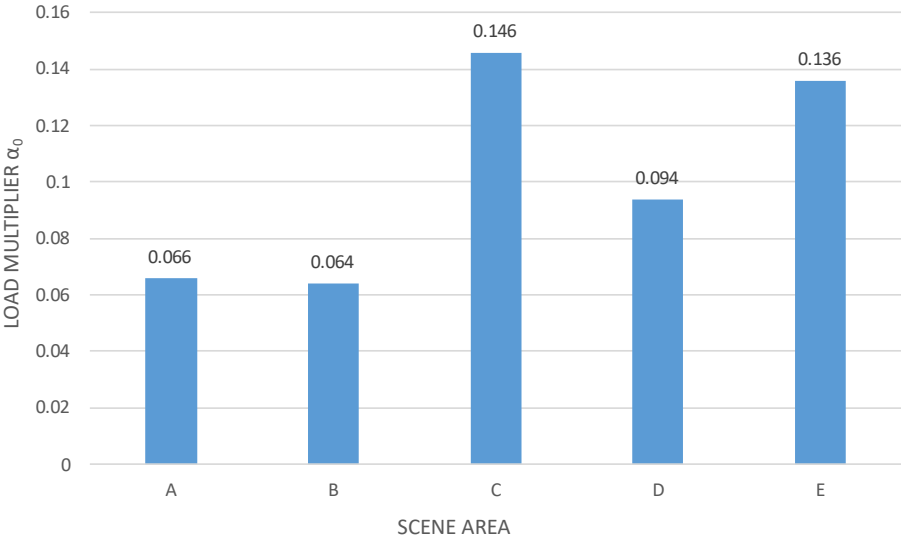


***Figure 4.11*** *- Histrogam with load multipier of each wall of the scene area*

This parameter is useful to calculate the capacity acceleration of the wall, in order to find the ratio between the capacity and request acceleration of the structure. The request acceleration is the acceleration provided by the NTC2018 that is equal to 0.183. The safety threshold for existing structures is equal to 80% because these have higher intrinsic vulnerability and consequently a lower percentage is admitted as a verification percentage. It turned out that all the portions are vulnerable because the different portions are not verified because do not reach the safety threshold equal to 80% (*Figure 4.12*). Except for wall C and E, for which it is different because for the case with the values furnished by NTC2018 the walls are verified.
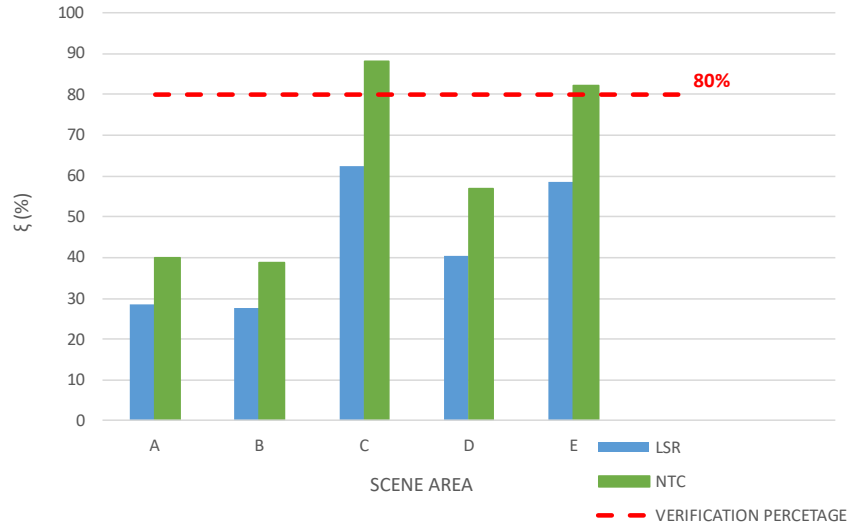
***Figure 4.12*** *- Comparison of the ratio between the capacity and the request acceleration for the local seismic response case (blue column) and the NTC2018 case (green column). The dashed line represents the verification percentage that is 80%*

In conclusion, the results highlight that all the walls of the scene area show a vulnerable behavior. In particular, the portion A and B appears to be the most vulnerable walls, while the portions C and E have a lower vulnerability with a capacity-demand ratio almost reaching the safety value (*Figure 4.13*). Moreover, it is necessary to stress that the linear kinematic approach represent a useful but still limited tool for the analysis of masonry wall, since the assumptions at the base of this approach are very conservative. In this case, several action may be implemented for a deeper investigation of the structural behavior, such as:

- performing Non-Linear kinematic analyses
- considering the mutual interaction of the different portions



***Figure 4.13*** *- Vulnerability of the different portions of the scene area*

# *DYNAMIC ANALYSIS*

The dynamic analysis investigates the dynamic behavior of the structure under ambient vibrations. From the recorded data are identified: experimental modal parameters in terms of natural frequencies, mode shapes that is the way in which the structure vibrates at a certain frequency and damping ratio which represent the degree in which the structure attenuates the vibrations.

Based on the experimental results a numerical model of the theater was constructed and calibrated. Then on the calibrated model a linear dynamic analysis was performed, using sets of accelerograms previously defined in chapter 3. The purpose is to define the response of the Roman Theater in terms of displacement and acceleration using a numerical modelling that uses a Finite Element Analysis (FEM).

## 5.1 Basics of structural dynamics

The structures can be divided in two different systems: Single Degree Of Freedom (SDOF) and Multi Degree Of Freedom (MDOF). The SDOF are the simplest structural systems in which the forces of inertia are concentrated in a single mass m, which can translate along a generic direction x (*Figure 5.1*). These are for example bridges or water tank.



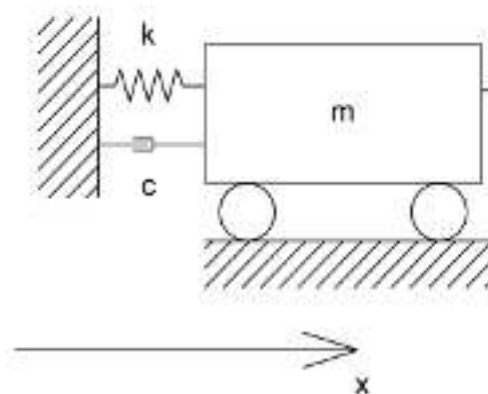**Figure 5.1** - *Schematic representation of a SDOF system*

The aim of the dynamics is to find the response of the system in terms of relative displacement of the mass m, solving the following equation:

$$m\ddot{x}(t) + c\dot{x}(t) + kx(t) = f(t)$$

this is the equation of the dynamic equilibrium where:

    f(t) is the external force

    k is the stiffness of the system

    c is the equivalent viscous damping coefficient

    $\dot{x}(t)$ is the velocity of the system

    $\ddot{x}(t)$ is the acceleration of the system

To find the solution of the equation the Duhamel's integral is used. It says that a generic forcing can be considered as a succession of small instants like short impulse dτ, each producing its own response. If the system is linear, it is possible to sum all these contributions to define the total response x(t) of the system:

$$x(t) = \frac{1}{m \, \omega_D} \int_0^t f(\tau) \, e^{-\xi \, \omega_N \, (t-\tau)} \, sin[\omega_D(t-\tau)] \, d\tau$$

where

    τ is the small instant

    $\omega_N$ is the natural frequency of the system equal to $\sqrt{\frac{k}{m}}$

    $\omega_D$ is the damped frequency equal to $\omega_D = \omega_N\sqrt{1-\xi^2}$

    ξ that is the damping ration, usually this value goes from 0.5% to 15%

More complex structures can be represented as systems with N degree of freedom. In this case, the equation that represent the behavior is:

$$M\ddot{x}(t) + C\dot{x}(t) + Kx(t) = f(t)$$

where

    M is the matrix of mass

    K is the matrix of the stiffness

    C is the matrix of damping

    x(t) is the vector of displacement

    f(t) is the vector of forces

In the case of undamped systems with free vibrations the equation is reduced to:

$$M\ddot{x}(t) + Kx(t) = f(t)$$

and the solution is:

$$x(t) = x\,e^{i\omega t}$$

The general solution can be written as:

$$(k - \omega^2 M)e^{i\omega t} = 0$$

and the non-trivial solution of the homogenous system can be obtained using the determinant:

$$\det |k - \omega^2 M| = 0$$

This equation gives an equation of grade n in $\omega^2$. The solutions are the eigenvalues $\omega$ that correspond to the natural frequencies of the undamped system. The lowest frequency is the fundamental one. If the eigenvalues are substituted inside the equation of motion, it is possible to obtain a series of eigenvectors $\psi$ that represents the vibration modes. The complete solution can be expresses with 2 matrices N x N. The eigenvector matrix $\phi$ that represents the n eigenvectors ($\psi$) of vibration modes:

$$\Phi = \begin{vmatrix} \vdots & \vdots & & \vdots & & \vdots \\ \psi_1 & \psi_2 & \cdots & \psi_i & \cdots & \psi_N \\ \vdots & \vdots & & \vdots & & \vdots \end{vmatrix}$$

The eigenvalues matrix $\Omega$ that represents the n natural frequencies ($\omega$) of the system associate to the vibration modes:

$$\Omega = \begin{vmatrix} \omega_1^2 & 0 & \vdots & 0 \\ 0 & \omega_2^2 & \vdots & 0 \\ \cdots & \cdots & \ddots & \cdots \\ 0 & 0 & \vdots & \omega_n^2 \end{vmatrix}$$

In the case of damped system with free vibration to find a solution is possible to diagonalize the matrix of mass and stiffness through the modal matrix $\phi$.

$$\phi^T M \phi = I$$

$$\phi^T K \phi = \Omega$$

I is the identity matrix and $\Omega$ is the eigenvalues matrix.

About C, it can be represented as a linear combination of M and K:

$$C = \alpha M + \beta K$$

$\alpha$ and $\beta$ are the Rayleigh coefficients.

It is possible to transform the equation of the system in modal coordinates:

$$x(t) \ = \ \phi \, u(t)$$

The equation becomes:

$$\ddot{u}(t) + (\alpha I + \beta \Omega)\dot{u}(t) + \Omega u(t) = 0$$

The equation can bel solved in the frequency domain using the Fourier transform.

## 5.2 Monitoring system and natural frequencies

Monitoring is very important for identifying damages and evaluating the performance of the structure under normal or particular conditions. In 2014, a monitoring system was installed on the scene area of the Roman Theater and the aim is the acquisition of vibration characteristics of the structure recorded by acceleration transducer, variation of the opening of fractures through displacement transducer and control of the inclination with inclinometers. These measurements are related to environmental parameters as temperature and relative humidity. On the wall four accelerometers have been places (*Figure 5.2*).
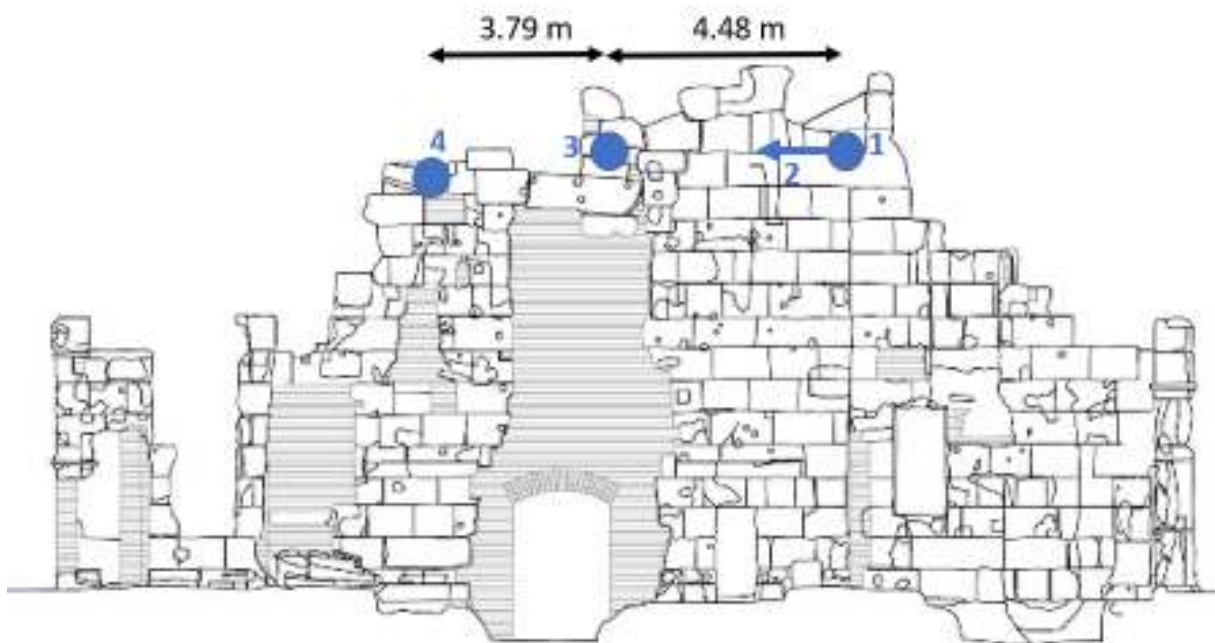


*Figure 5.2 - Position and distance of the monitoring sensors*

The system is based on trigger-based data acquisition methodology; it means that the recordings of vibrations are carried out at regular time intervals (12h or 24h) or when a preestablished threshold level is exceed both in time and frequency domain. In Figure 5.2 it is possible to observe the positions of the accelerometers, the sensors 1 and 2 are placed at the top of the septum constituting the scene, S1 measures out-of-plane acceleration while S2 measures those

in-plane. S3 is in the middle upper part of the wall and measures out-of-plane acceleration. S4 is fixed in a brick block on the left opening of the scene at the top and measures out-of-plane acceleration.

Using an experimental approach is possible to determine the natural frequencies of the structure; to do that the software ARTeMIS is used. To make the analysis the first thing is to recreate the geometry of the scene area; in this case the geometry is not the real one but is an approximation (*Figure 5.3*). This because the aim of this analysis is to understand the vibrational modes of the wall.
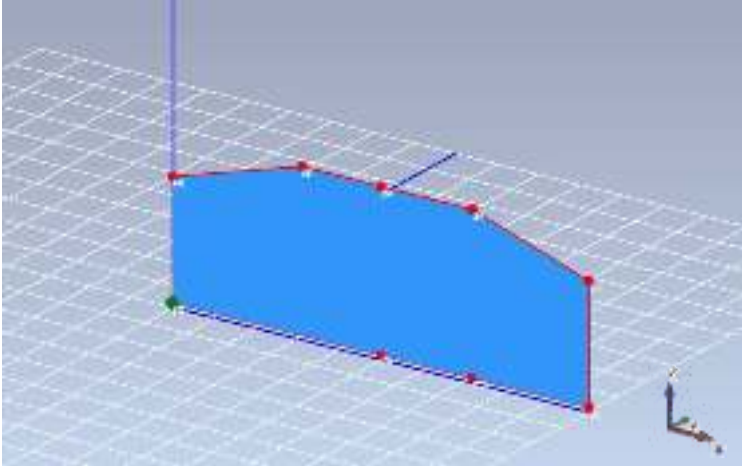


*Figure 5.3 - Approximative geometry of the wall of the scene area for the experimental analysis*

The input used for the analysis are five different acquisitions recorded by the sensors. To the data a bandpass filter is applied with a minimum frequency of 0.5Hz and a maximum frequency of 49Hz. The estimators used for the analysis are the EFDD and SSI, in particular the UPC, PC and UPCX. The result is a Singular Values of Spectral Densities (SVD) graph, which each peak corresponds to a vibrational mode of the structure (*Figure 5.4*).



*Figure 5.4 - Singular Values of Spectral Densities (SVD) graph. The vertical red lines highlight the firsts modes of vibration of the wall of the scene area.*

In *Tables 5.1* are reported all the results obtained from the different estimators for each recording.

**Table 5.1** - *Natural frequencies of the structure obtained from the experimental analysis*

### Record 1

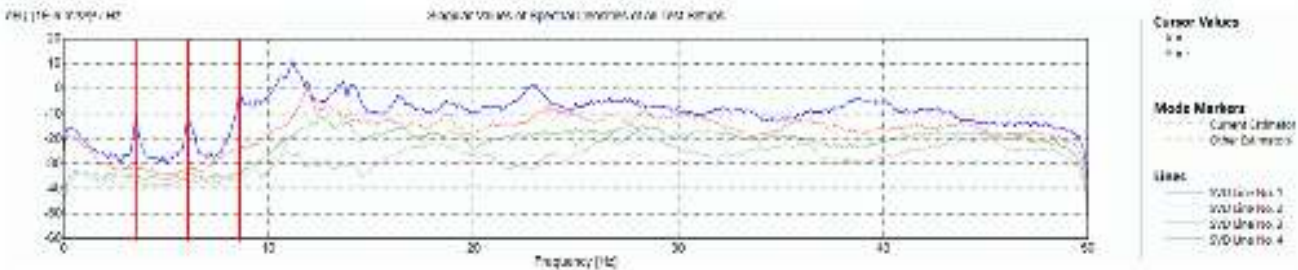|            | M1  | M2  | M3  |
|------------|-----|-----|-----|
| EFDD       | 3.5 | 6.1 | 8.7 |
| SSI – UPC  | -   | -   | 8.7 |
| SSI – PC   | -   | -   | 8.7 |
| SSI – UPCX | -   | -   | 8.7 |

### Record 2

|            | M1  | M2  | M3  |
|------------|-----|-----|-----|
| EFDD       | 3.5 | 6.2 | 8.7 |
| SSI – UPC  | -   | -   | 8.7 |
| SSI – PC   | -   | -   | 8.6 |
| SSI – UPCX | -   | -   | 8.7 |

### Record 3

|            | M1  | M2  | M3  |
|------------|-----|-----|-----|
| EFDD       | 3.5 | 6.1 | 8.7 |
| SSI – UPC  | -   | -   | 8.7 |
| SSI – PC   | -   | -   | 8.6 |
| SSI – UPCX | -   | -   | 8.7 |

### Record 4

|            | M1  | M2  | M3  |
|------------|-----|-----|-----|
| EFDD       | 3.5 | 6.1 | 8.7 |
| SSI – UPC  | -   | -   | 8.7 |
| SSI – PC   | -   | -   | 8.6 |
| SSI – UPCX | -   | 6.2 | 8.6 |

*Record 5*

|        | M1  | M2  | M3  |
|--------|-----|-----|-----|
| EFDD   | 3.5 | 6.1 | 8.7 |
| SSI – UPC  | -   | -   | 8.8 |
| SSI – PC   | -   | -   | 8.7 |
| SSI – UPCX | -   | -   | 8.6 |

From the *Tables 5.1* is possible to retrieve the frequencies of the different vibrational modes:

- Mode 1: f = 3.5 Hz

- Mode 2: f = 6.1 Hz

- Mode 3: f = 8.7 Hz

About the SSI estimators, these do not recognize the first and the second vibrational mode, except for record 4 in which also the second one was identified. These modes are showed in *Figure 5.5*.

1ˢᵗ mode          f = 3.5 Hz



2ⁿᵈ mode          f = 6.1 Hz

3<sup>rd</sup> mode $\quad$ f = 8.7 Hz
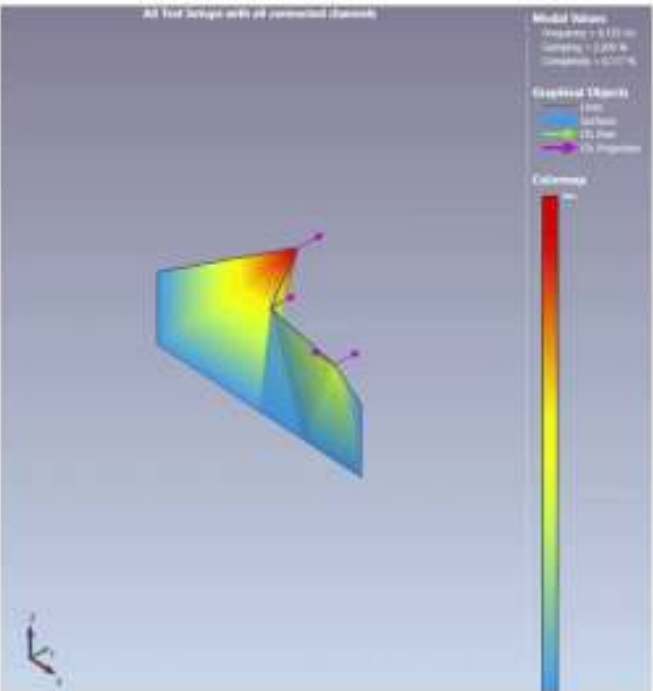


***Figure 5.5*** *- Representation of the 1ˢᵗ, 2ⁿᵈ and 3ʳᵈ vibrational modes of the scene area of the Roman Theater*

The first mode of vibration is the fundamental one, for the scene area is 3.5 Hz and its period corresponds to:

$$T = \frac{1}{f} = \frac{1}{3,5 \ Hz} = 0.28s$$

Looking *Figure 5.6* the fundamental frequency of the structure coincides with the plateau of the representative response spectrum of the Roman Theater site and the extreme case of 1117 earthquake. This means that the fundamental mode coincides with the maximum spectral acceleration of these two cases. It represents the worst case because the maximum displacement and acceleration will be recorded. Different for the case of the local response with the seven accelerograms in which the fundamental frequency does not correspond to the plateau: this implies that the acceleration and displacement will not be the maximum that could be recorded.
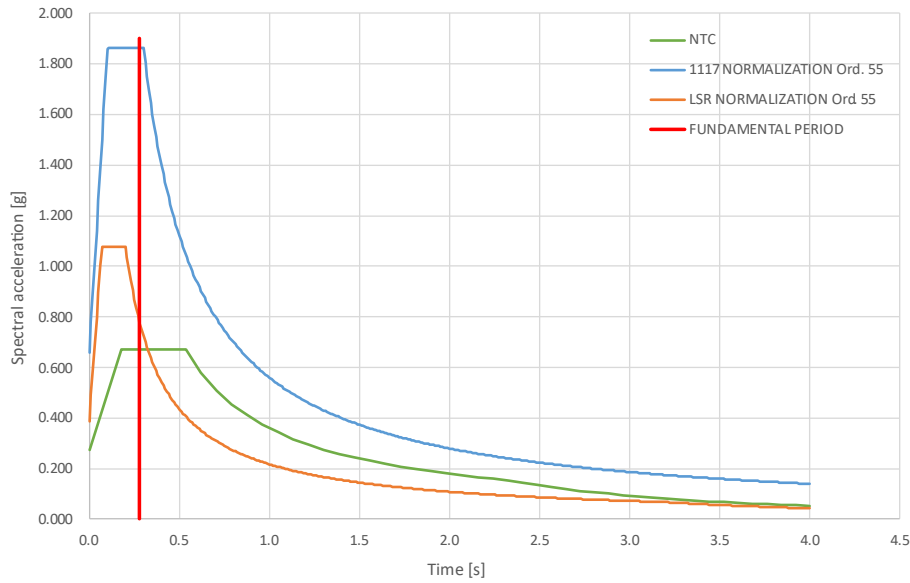
67

***Figure 5.6*** - *Comparison between the normalized spectra (following the Order No. 55) of the earthquake of 1117 (blue), the set of accelerogram (orange) and site with soil E and topography T1 (green). The red line represents the period of the resonance frequency*

## 5.3 Numerical analyses

### 5.3.1 Model calibration

For the dynamic analysis the software Straus7 was used and it utilizes a numerical model. At first a dynamic identification with a numerical model was done, in order to create a calibrated model for the linear dynamic analysis. The calibration consists in slightly modifying the stiffness value of the structure (within the values provided by the standard), knowing that:
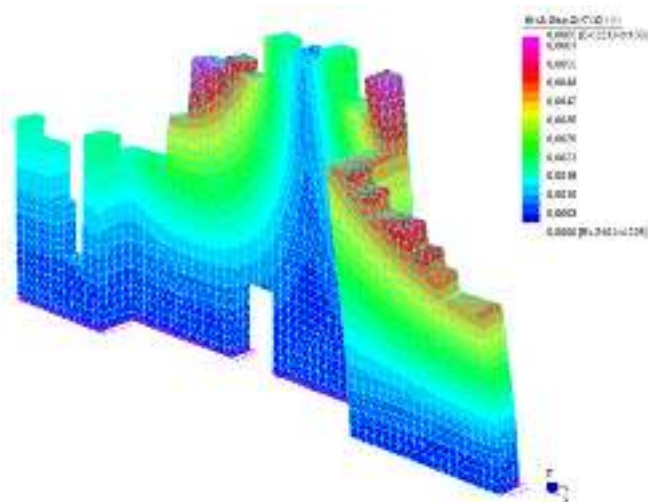
$$f = \sqrt{\frac{k}{m}}$$

in order to obtain vibration frequencies similar to those obtained before. The first three vibrational modes are reported in *Figure 5.7*.

1st mode          f = 3.45 Hz
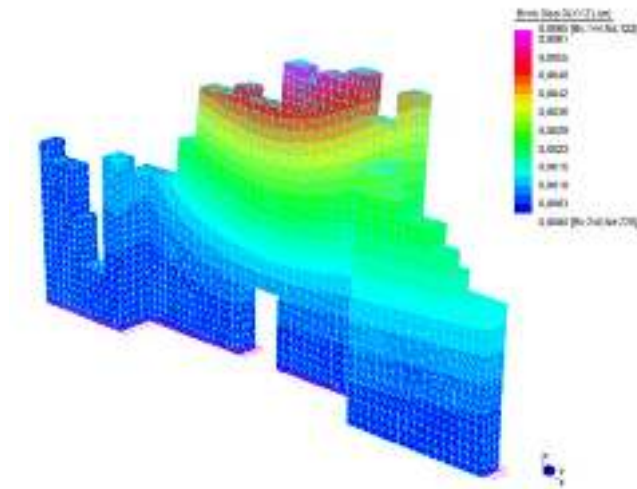


2nd mode          f = 5.84 Hz
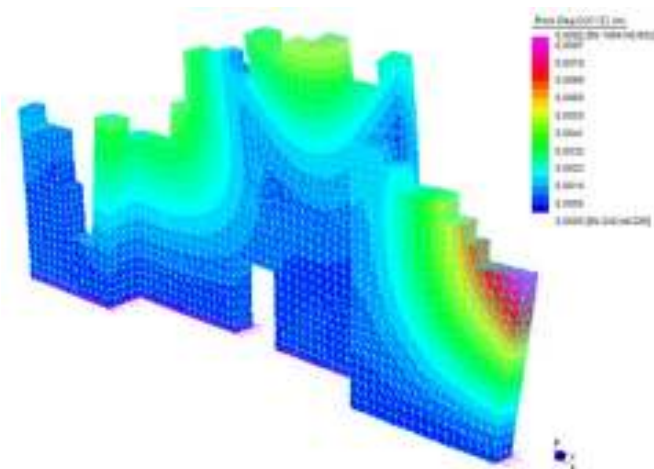


3rd mode          f = 9.47 Hz



*Figure 5.7 - Representation of the 1st, 2nd and 3rd vibrational modes of the scene area of the Roman Theater*

It is possible to make a comparison between the vibrational modes obtained from the experimental analysis and from the numerical analysis, to see how different the vibrational modes are (*Table 5.2*).

*Table 5.2* - *Comparison between the frequencies of vibrational modes calculated with the experimental and numerical approach. The third column calculates the error between the exact value and the approximated one*

|  | EXPERIMENTAL | NUMERICAL | ERROR (%) |
|---|---|---|---|
| 1$^{ST}$ MODE | 3.5 Hz | 3.45 Hz | 1.45% |
| 2$^{ND}$ MODE | 6.1 Hz | 5.84 Hz | 4.45% |
| 3$^{RD}$ MODE | 8.7 Hz | 9.47 Hz | 8.13% |

The values calculated with the experimental approach are slightly different respect to the ones obtained with the numerical model; in particular the third mode is the one that have the higher error percentage, about 8%.

### 5.3.2 Linear dynamic analyses

After the dynamic identification the linear dynamic analysis will be performed. It consists in the study of the dynamic behavior of the structure in terms of displacement and acceleration. The inputs are the three accelerogram obtained in chapter 3 (*Figure 3.15*), applied in the out-of-plane direction (y direction). In particular, in this analysis the accelerograms used are cut; in this way only the part with the maximum acceleration will be study, given that is the one that produces more damages (*Figure 5.8*). The results will be graphs both for acceleration and displacement in a point in the upper part of the wall, at node 2026 (*Figure 5.9*).

## CUT AVERAGE LSR ACCELEROGRAM
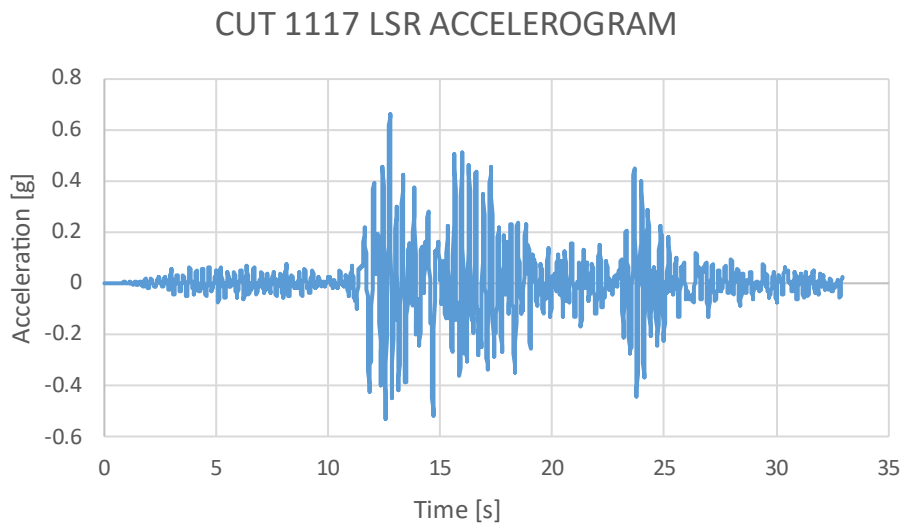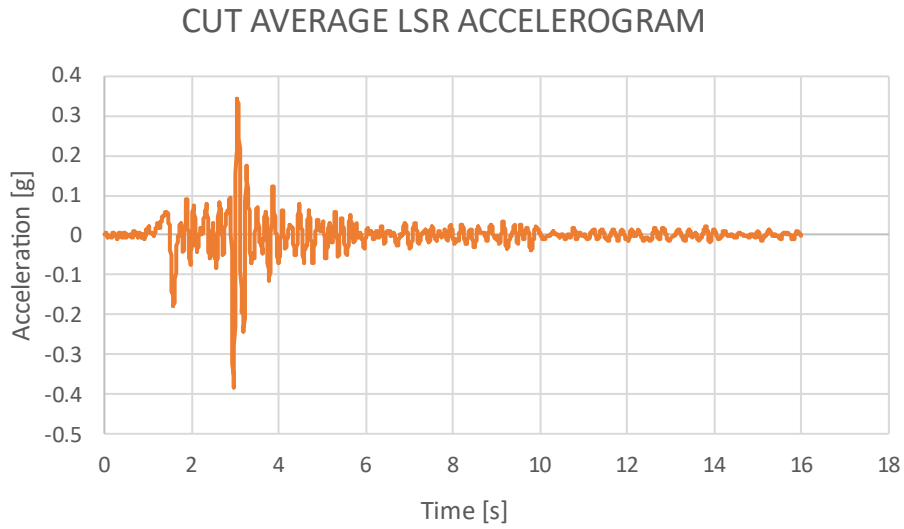


## CUT 1117 LSR ACCELEROGRAM
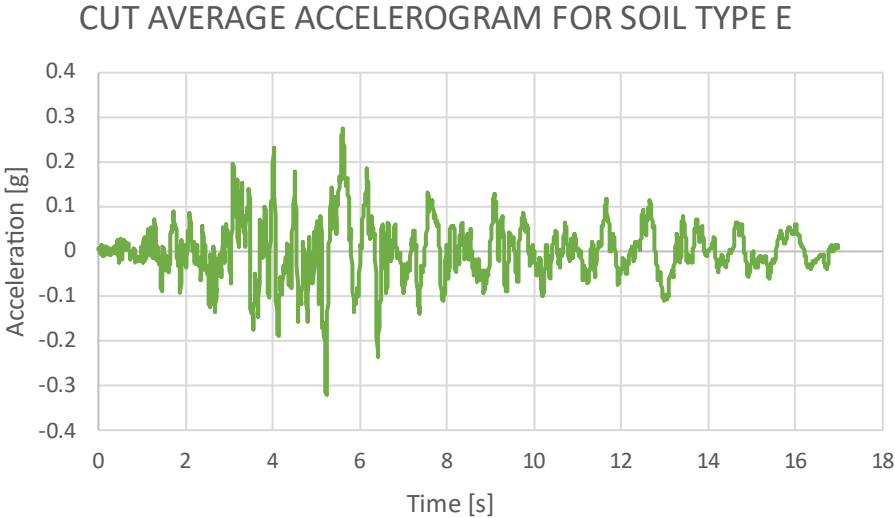


*Figure 5.8* - *Three input accelerograms used for the linear dynamic analysis. The first one is the accelerogram spectral compatible to the NTC2018. The second one was obtained from the local response analysis of the set of seven accelerograms. The third one is the result obtained from the local seismic response analysis using an earthquake like the Verona 1117*
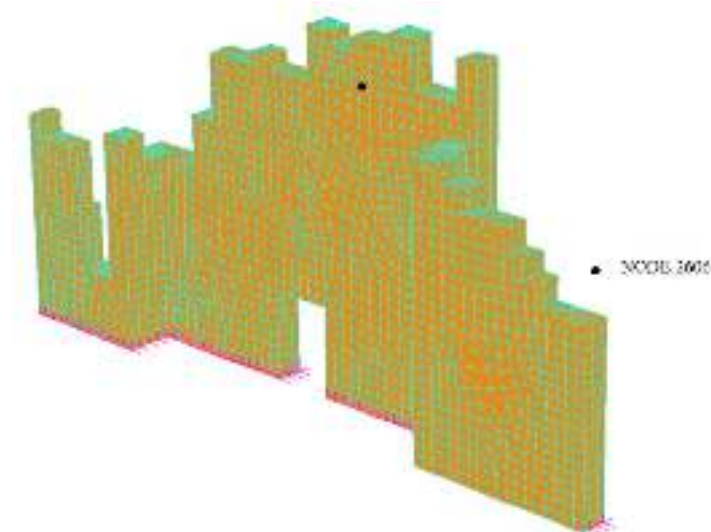


*Figure 5.9* - *Calibrated model of the scene area of the Roman Theater. The black dot (node 2606) is the point in which will be extrapolated all the results*

## SOIL TYPE E ACCORDING TO NTC2018

As already said, the accelerogram used as input is an average accelerogram spectral compatible to the response spectra of soil type E. For each section will be showed the behavior of the wall in terms of relative displacement and relative acceleration in the upper part of the structure. Another comparison that will be discussed is between the acceleration at the base and the one recorded at the top, this is an important aspect that show how much the structure could amplify the seismic action.


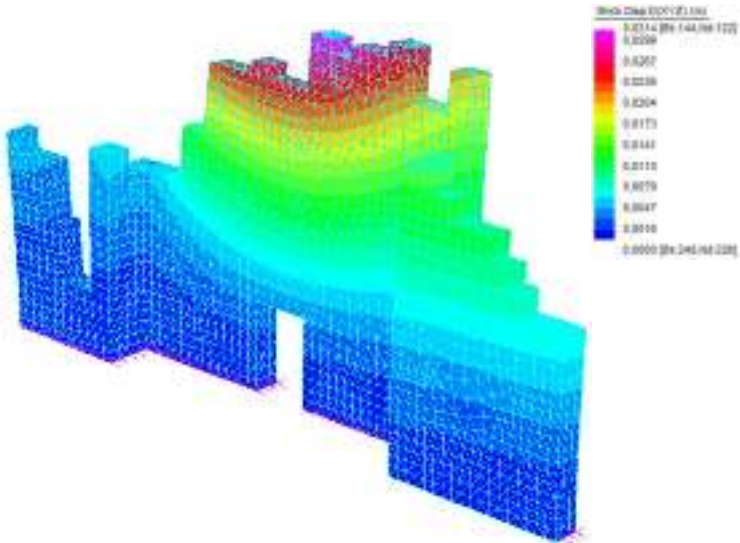
*Figure 5.10 - Maximum displacement of the wall subjected to an earthquake that the standards attend for a soil type E*
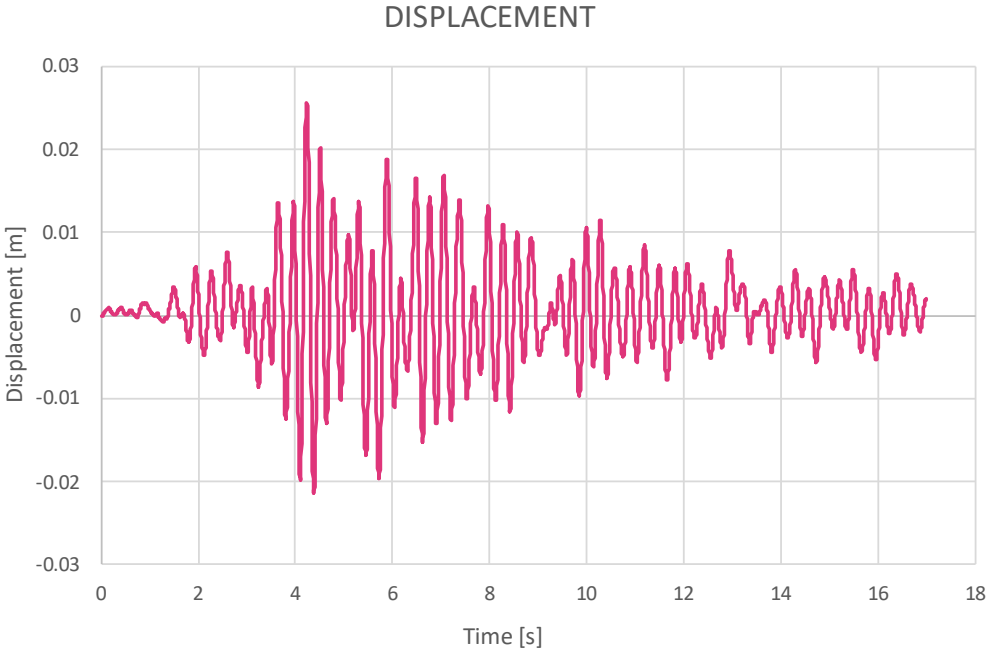


*Figure 5.11 – Displacement at node 2606 of the wall subjected to an earthquake that the standards attend in a soil type E*
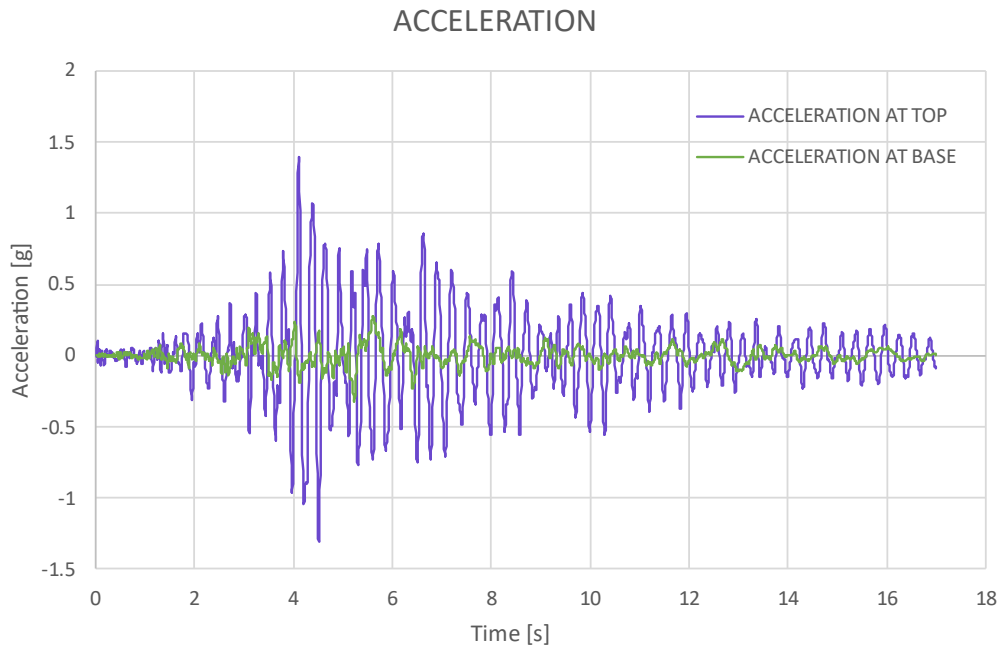
ACCELERATION

**Figure 5.12** - *Acceleration at node 2606 of the wall subjected to an earthquake that the standards attend in a soil type E. It is compared with the accelerogram used as input (green)*

The maximum displacement recorded at the top of the wall is 0.025m and the maximum acceleration is 1.39g.

## AVERAGE ACCELEROGRAM FROM LOCAL SEISMIC RESPONSE ANALYSIS

In this case the accelerogram is the average obtained from the set of seven accelerogram used for the local seismic response analysis according to the standards.
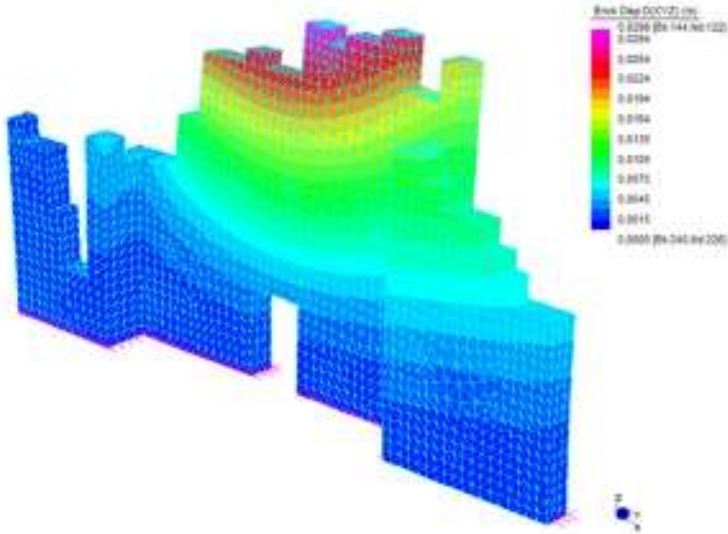


***Figure 5.13*** *- Maximum displacement of the wall subjected to an earthquake obtained from the local seismic response analysis*



***Figure 5.14*** *– Displacement at node 2606 of the wall subjected to an earthquake obtained from the local seismic response analysis*

***Figure 5.15*** - *Acceleration at node 2606 of the wall subjected to an earthquake obtained from the local seismic response analysis. It is compared with the accelerogram used as input (orange)*

The maximum displacement recorded at the top of the wall is 0.024m and the maximum acceleration is 1.55g.

## 1117 EARTHQUAKE

The input is the earthquake of 1117 obtained after the seismic response analysis.
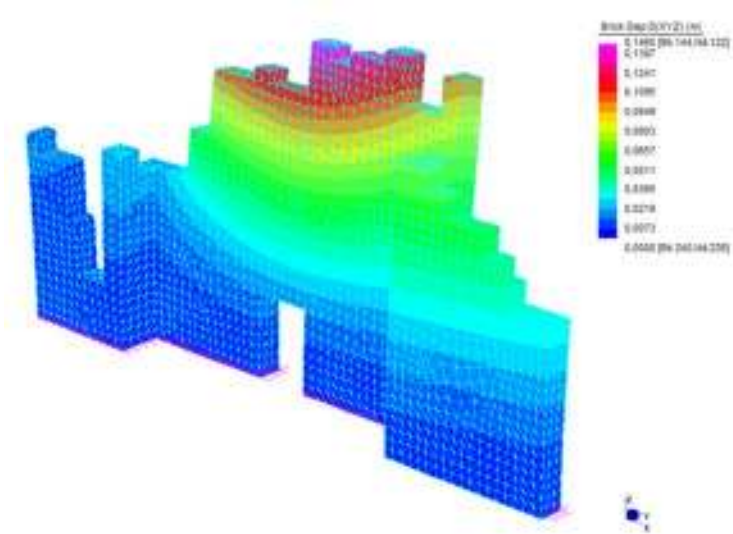


***Figure 5.16*** *- Maximum displacement of the wall subjected to 1117 earthquake*



***Figure 5.17*** *– Displacement at node 2606 of the wall subjected to 1117 earthquake*

**ACCELERATION**

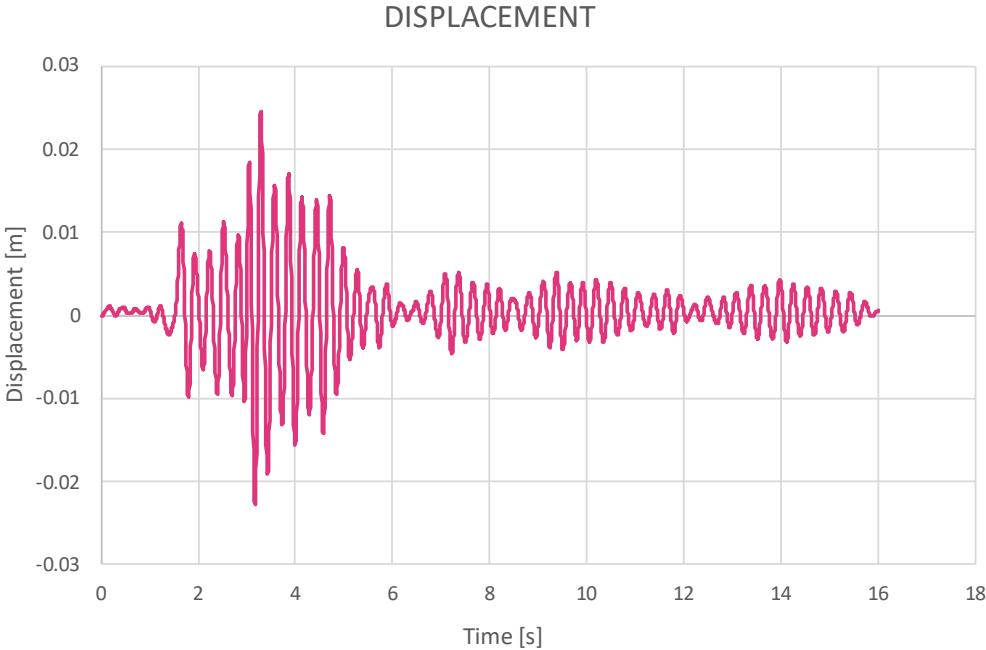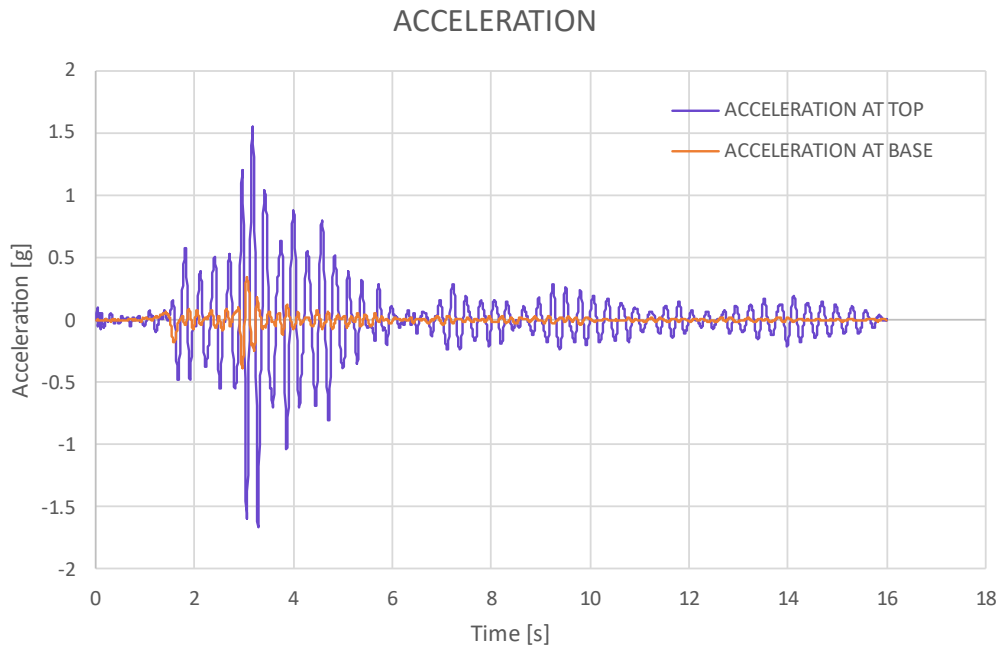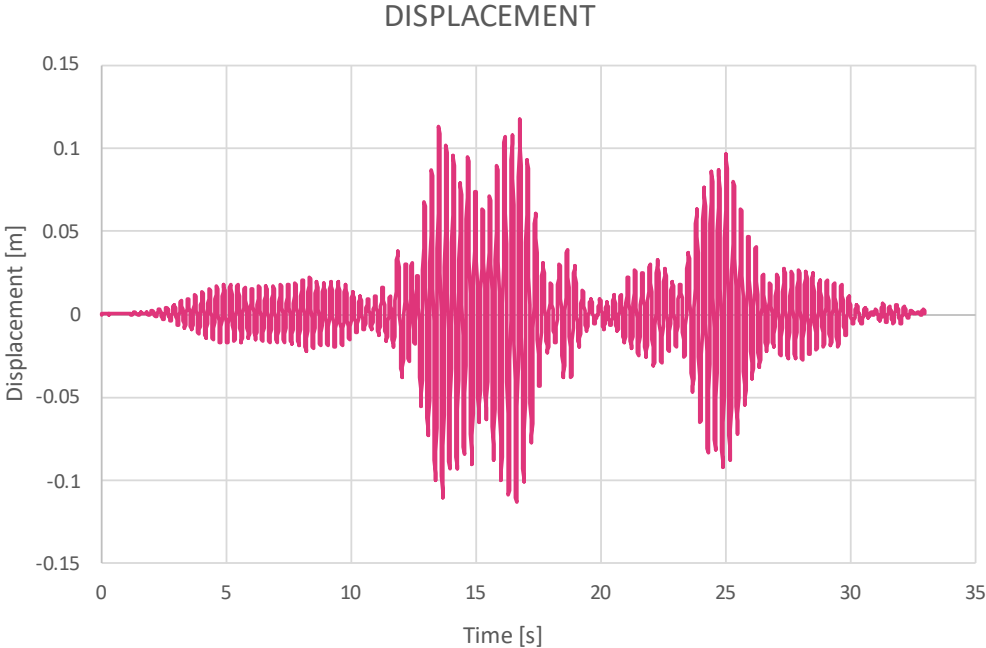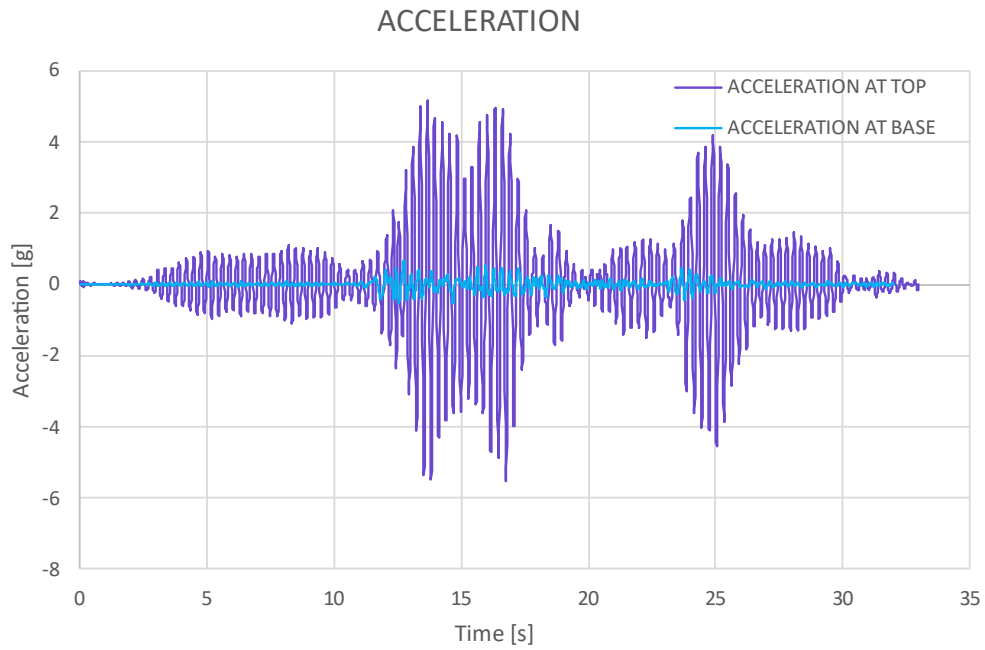*Figure 5.18 - Acceleration at node 2606 of the wall subjected to an earthquake obtained from the local seismic response analysis. It is compared with the accelerogram used as input (blue)*

The maximum displacement recorded at the top of the wall is 0.117m and the maximum acceleration is 5.16g.

Concluding, it is possible to make a summary table with all the results obtained by the dynamic analysis (*Table 5.3*).

*Table 5.3 - Summary table with the relative displacements and relative accelerations obtained from each analysis in the upper part of the wall*

|  | NTC | RSL | 1117 |
|---|---|---|---|
| DISPLACEMENT (m) | 0.025 | 0.024 | 0.117 |
| ACCELERATION (g) | 1.39 | 1.55 | 5.16 |

From the results it is possible to see that the worst response is in the case of the earthquake of 1117. The case of the seismic code parameters and the analysis with the seven accelerograms have more or less the same results. This because looking at the response spectra of the local response analysis of the set of accelerogram, the fundamental frequency of the structure does not coincide with the plateau but coincide to an acceleration that is close to the plateau of the response spectra of a soil type E (*Figure 5.6*). Indeed, for the first analysis the wall is subjected to a displacement around 2.5cm, otherwise the second the displacement is 2.4cm. Very different is the case of the 1117 earthquake that produced a maximum displacement of the structure about 11.7cm and reaches a maximum acceleration of 5g. Bigger is the displacement of the structure and bigger is the earthquake: the 1117 earthquake is the greatest event occurred in Verona. Looking at the accelerations, is possible to observe that there is an amplification of those respect to the accelerations used as input. This means that the presence of the structure produces an amplification itself of the seismic input.

# *CONCLUSIONS*

The thesis work highlighted through a multidisciplinary approach the effects of the soil to a seismic action and consequently the response of the structure to that event.

From the geological and geophysical analyses was seen that the Roman Theater area is characterized by a soil type E (second the Italian NTC18 and Eurocode 8), where the first meters are composed by silty sandy gravel with variable thickness and the bedrock is very shallow. With the local seismic response analysis, it was discovered that the presence of this soft layer generates an amplification of the seismic motion in the area. This is an important aspect to consider because even if the bedrock is shallow, the acceleration recorded at the surface is higher than the one at the hard basement. Comparing the results with the values provided by the Italian seismic code for that site, it is evident that the method used is more rigorous. The expected accelerations by the NTC2018 are less compared to the ones that could be recorded in a real case, like a general earthquake produced at the bedrock or an extreme case like 1117 Verona earthquake.

From the dynamic identification the first 3 natural frequencies were found, in order to make a calibrated model for the dynamic analysis. The fundamental frequency of the structure coincides with the plateau of the representative response spectrum of the Roman Theater site and the extreme case of 1117 earthquake. This means that the fundamental mode coincides with the maximum spectral acceleration of these two cases and it represents the worst case because the maximum displacement and acceleration will be recorded. Different for the case of the local response with the seven accelerograms in which the fundamental frequency does not correspond to the plateau, this implies that the acceleration and displacement will not be the maximum that could be recorded.

The structural analysis of the Roman Theater, divided in kinematic and dynamic, is useful to understand the behavior of the wall of the scene area in the different situations. With the kinematic analysis, the local mechanisms were studied. The load multiplier is the fundamental parameter that produces the activation of the mechanism. It is useful to calculate the capacity acceleration of the wall, in order to find the ratio between the capacity and request acceleration of the structure. It turned out that all the portions are vulnerable because the different portions are not verified because do not reach the safety threshold equal to 80%. Except for wall C and E, for which it is different because for the case with the values furnished by NTC2018 the walls are verified. This method is a useful tool but for the analysis of masonry wall a deeper

investigation is required, for example performing a Non-Linear kinematic analysis or considering the mutual interaction of the different portions.

With the dynamic analysis it was possible to understand the maximum displacement and the maximum acceleration at which the structure could be subjected. Doing a comparison between the three cases it is possible to see that the one with the seismic code parameters has the lower values. It is possible to observe that this case has very similar results to the analysis with the seven accelerograms. This because, as already said, looking at the response spectra of the local response analysis of the seven accelerogram, the fundamental frequency of the structure does not coincide with the plateau. The worst case is the earthquake of 1117, that produces a displacement to the structure of 11cm. Indeed, greater is the earthquake and bigger will be the damages produced. Also, the acceleration is very high for this case, in particular is possible to observe, in the three cases, a difference between the acceleration recorded at the base and the one at the top: the presence of the structure could amplify the seismic motion.

The Verona Roman Theater has a cultural importance and in the past different natural disaster reduced its stability. In Verona the biggest event was the 1117 earthquake, that produced several damages. The structure was built above the Adige Line, which is also defined as the maximum seismogenic potential for the Lessini-Schio district, that could generate earthquakes up to a magnitude of 6.7. For this reason, it is necessary an accurate monitoring system and ongoing maintenance work to guarantee the safety of the structure and accessibility to one of the most panoramic historical monuments of the city.

# BIBLIOGRAPHY

Bolla M., Il Teatro Romano di Verona e le sue sculture. Verona (2010).

Da Porto F., Lorenzoni F., Caprino A., Bonaldo G. Acquisizione di elementi e di documenti dello stato dell'arte. (2022).

Da Porto F., Stefani C., Boaga J., Lorenzoni F., Caprino A., Bonaldo G. Integrazione delle informazioni relative allo stato dell'arte. (2022).

Dal Degan D. Verifica del rischio sismico, riduzione della vulnerabilità e restauro della Cattedrale di Santa Maria Assunta. (2022).

Dal Ronco N. Identificazione strutturale del Teatro Romano di Verona mediante monitoraggio statico e dinamico. Tesi di laurea, Università degli Studi di Padova, Dipartimento di Ingegneria Civile Edile Ambientale. Padova (2015).

Darti G. F. Indagine geologica geotecnica sui terreni interessati dal progetto di ristrutturazione del museo archeologico presso il Teatro Romano di Verona siti in via Rigaste Redentore in Comune di Verona. (2012).

Fabbrocino G., Rainieri C., Verderame G. M. L'analisi dinamica sperimentale e il monitoraggio delle strutture esistenti.

Franzoni L., Lampronti G. Il Teatro Romano: la storia e gli spettacoli. Verona. (1988).

Furlani S. Vulnerabilità strutturale del Teatro Romano di Verona mediante modellazione analitica e numerica. Tesi di laurea, Università degli Studi di Padova, Dipartimento di Ingegneria Civile Edile Ambientale. Padova (2015).

Modena C., Lorenzoni F., Caldon M. Relazione conclusiva sull'installazione del sistema di monitoraggio strutturale presso il Teatro Romano. (2015).

Molinari M. Analisi di vulnerabilità sismica del Teatro Romano di Verona. Teso di laurea, Università degli Studi di Padova. Padova (2010).

Mufti, Guidlines for Structural Health Monitoring. University of Manitoba, ISIS Canada (2001).

Nori L., Di Marcantonio P. Manuale pratico di risposta sismica locale. Dal sismogramma allo spettro di progetto con REXEL e STRATA. 78 p. (2014).

Sugan, M. Peruzza, L. Distretti sismici del Veneto. Bollettino di Geofisica Teorica ed Applicata. (2011).

Valdinoci M., Bertini D. Interventi tesi alla verifica del rischio sismico, riduzione della vulnerabilità e restauro. (2022).

Vinci M. Metodi di calcolo e tecniche di consolidamento per edifici in muratura. Secondo il D.M 17/01/2018 e Circolare 7/2019. 227 p. (2019).


Aggiornamento per le "Norme tecniche per le costruzioni", (2018). Roma: Ministero delle infrastrutture e trasporti.

Ordinanza n. 55 del 24 aprile 2018. Appendice 1 - Regolarizzazione di uno spettro ottenuto con gli studi di MS3.

# ATTACHMENTS

Figure 1.2 - https://www.verona.net/it/monumenti/teatro_romano.html

Figure 1.3 - https://www.culturaveneto.it/it/la-tua-regione/patrimonio-mondiale-unesco-in-veneto

Figure 1.4a - Da Porto F., Lorenzoni F., Caprino A., Bonaldo G. Acquisizione di elementi e di documenti dello stato dell'arte. (2022)

Figure 1.4b - Da Porto F., Lorenzoni F., Caprino A., Bonaldo G. Acquisizione di elementi e di documenti dello stato dell'arte. (2022)

Figure 1.4b - Da Porto F., Lorenzoni F., Caprino A., Bonaldo G. Acquisizione di elementi e di documenti dello stato dell'arte. (2022)

Figure 1.5 - Valdinoci M., Bertini D. Interventi tesi alla verifica del rischio sismico, riduzione della vulnerabilità e restauro. (2022)

Figure 1.6 - De Zanche V., Sorbini L. Carta geologica del territorio del Comune di Verona. Verona, (1977).

Figure 1.7 - Sugan M., Peruzza L. Distretti sismici del Veneto. Bollettino di Geofisica Teorica ed Applicata. (2011)

Figure 1.8 - https://diss.ingv.it/

Figure 1.9 - http://sgi.isprambiente.it/ithaca/viewer/index.html

Figure 2.1 - Da Porto F., Lorenzoni F., Caprino A., Bonaldo G. Acquisizione di elementi e di documenti dello stato dell'arte. (2022)

Figure 2.2 - Da Porto F., Lorenzoni F., Caprino A., Bonaldo G. Acquisizione di elementi e di documenti dello stato dell'arte. (2022)

Figure 2.4 - https://www.researchgate.net/figure/Wenner-electrode-configuration_fig4_3403 79334

Figure 2.5 - Tosi G. Gli edifici per spettacolo di Verona

Figure 2.6 - Valdinoci M., Bertini D. Interventi tesi alla verifica del rischio sismico, riduzione della vulnerabilità e restauro. (2022)

Figure 2.7 - Valdinoci M., Bertini D. Interventi tesi alla verifica del rischio sismico, riduzione della vulnerabilità e restauro. (2022)

Figure 2.9 - https://www.gmpe.it/terremoti/onde-sismiche

Figure 2.10 - https://www.gmpe.it/terremoti/onde-sismiche

Figure 2.11 - https://www.gmpe.it/terremoti/onde-sismiche

Figure 2.12 - Socco L. V., Strobbia C. Surface-wave method for near-surface characterization: a tutorial. (2004)

Figure 2.13 - Tosi G. Gli edifici per spettacolo di Verona

Figure 3.3 – Nori L., Di Marcantonio L. Manuale pratico di risposta sismica locale. Dal sismogramma allo spettro di progetto con REXEL e STRATA. 87 p. (2014)

Figure 4.2 - Vinci M. Metodi di calcolo e tecniche di consolidamento per edifici in muratura. Secondo il D.M 17/01/2018 e Circolare 7/2019. 227 p. (2019)

Figure 4.3 - Vinci M. Metodi di calcolo e tecniche di consolidamento per edifici in muratura. Secondo il D.M 17/01/2018 e Circolare 7/2019. 227 p. (2019)

# *RINGRAZIAMENTI*

*Al mio relatore, Prof. Jacopo Boaga che mi ha dato la possibilità di approfondire questa tematica così interessante e si è sempre dimostrato disponibile nel risolvere i problemi incontrati durante il percorso.*

*All' Ing. Filippo Lorenzoni e Dott. Amedeo Caprino che mi hanno seguita nello svolgimento delle analisi e sono sempre stati disponibili per spiegazioni con l'opportunità di scoprire nuovi aspetti di questo argomento.*

*Ai miei amici, a quelli che ci sono sempre stati e a quelli appena conosciuti. Mi hanno accompagnata in questo percorso pronti a darmi sempre una parola di conforto, ad incoraggiarmi per affrontare ogni difficoltà.*

*Ai miei parenti che mi hanno sempre sostenuta e sono sempre stati al mio fianco a festeggiare ogni piccolo traguardo.*

*Ai miei genitori, sempre presenti in questo breve ma intenso percorso. A mia mamma che con il suo modo deciso mi ha sempre riportata sulla strada giusta e motivata a continuare. A mio papà, uomo di poche parole ma che con un sorriso e il suo sguardo mi ha sempre comunicato il suo sostegno.*

*A Carloalberto, persona speciale che mi ha insegnato tanto. Giorno dopo giorno mi hai accompagnata verso questo traguardo speciale. Hai saputo consigliarmi in ogni momento e aiutata rialzarmi ad ogni sconfitta.*

*A me, alla me che non pensava di riuscirci. Ti ringrazio per la costanza che ti ha contraddistinto e quella voglia di fare che ti si legge negli occhi. Sii sempre così, sono fiera di te.*

*A tutti voi…*

*Grazie*

*Eleonora*